

RADIATIVE IGNITION OF THERMALLY THICK MEDIA

A THESIS

Presented to

The Faculty of the Division
of Graduate Studies

By

Gary Lee Matson

In Partial Fulfillment

of the Requirements for the Degree

Master of Science in Mechanical Engineering

Georgia Institute of Technology

March, 1976

7-254
RADIATIVE IGNITION OF THERMALLY THICK MEDIA

Approved:

P. Durbetaki, Chairman

A. V. Larson

E. A. Powell

W. C. Tincher

Date approved by Chairman: 2/25/1976

ACKNOWLEDGMENTS

I would like to extend my sincere appreciation to my thesis advisor, Dr. Pandeli Durbetaki, for his guidance and helpful suggestions throughout the duration of this investigation. I would also like to thank the other members of the reading committee for their interest and comments concerning this thesis.

I wish to express my appreciation to the School of Mechanical Engineering for the opportunity to conduct this research and to the technical staff for its many contributions. Special appreciation is extended to Mr. Gene Clopton for his invaluable help in the design and installation of the LITA electrical system.

I would also like to thank the National Science Foundation for its support of this work.

Finally, I wish to express my appreciation to my parents for their encouragement, and to my wife, Cath, for her support and understanding during the course of this work.

TABLE OF CONTENTS

	Page
ACKNOWLEDGMENTS.	ii
LIST OF TABLES	v
LIST OF ILLUSTRATIONS.	vi
NOMENCLATURE	viii
SUMMARY.	ix
Chapter	
I. INTRODUCTION.	1
Relevance of Flammability Research	
Background of Research Program	
Thesis Objectives	
II. EXPERIMENTAL APPARATUS.	6
System Characterization	
The Supporting Structure	
The Radiant Heater Stack and Heater Power Supply	
The Radiant Heater Stack	
The Heater Power Supply	
The Shutter Systems	
The Sample Holder Assembly and Disposal System	
Instrumentation	
Instrumentation for Exposure Control	
Instrumentation for Flame Detection	
The Control Panel	
The Exhaust System	
III. EXPERIMENTAL PROCEDURE.	42
Measurement of the Heat Flux of the Radiant	
Heater Stack	
Measurement of the Heater Current	
Measurement of Shutter Velocities	
Fabric Sample Preparation	
Wood Sample Preparation	

Chapter	Page
Ignition Time and Ignition Frequency Measurement Procedures	
Ignition Time Measurement Procedures	
Ignition Frequency Measurement Procedures	
IV. RESULTS AND DISCUSSION.	55
The Heat Flux Measurement of the Radiant Heater Stack	
Shutter Velocity Tests	
Total Heater Current Measurements	
Summary of Fabric Ignition Time Measurement	
Summary of Fabric Ignition Frequency Tests	
Summary of Wood Ignition Time Measurements	
V. CONCLUSIONS AND RECOMMENDATIONS	79
Summary of Accomplishments	
Conclusions on Observations and Recommendations for Further Work	
Appendix	
A. ASSEMBLY DRAWINGS	84
B. SCHEMATICS OF THE LITA ELECTRICAL SYSTEM.	88
C. FABRIC PROPERTIES AND DATA.	96
D. WOOD PROPERTIES AND DATA.	100
E. OPERATING CHARACTERISTICS OF THE RADIANT HEATER STACK	104
BIBLIOGRAPHY	107

LIST OF TABLES

Table	Page
C.1. Thermophysical Properties of the Fabric Samples Tested.	97
C.2. Summary of Ignition Time Measurements on Fabric Samples Using LITA and RITA.	98
D.1. Thermophysical Properties of the Wood Samples Tested.	101
D.2. Summary of Ignition Time Measurements on Thermally Thick Materials, 15.2 cm x 15.2 cm Samples	102
E.1. Total Heater Current Versus Heater Voltage. . . .	105

LIST OF ILLUSTRATIONS

Figure	Page
1. Overall View of the Large Ignition Test Apparatus and Associated Instrumentation.	8
2. Assembly Drawing of LITA Without the Exhaust Hood, Front View.	9
3. Assembly Drawing of LITA, Top View.	10
4. View of LITA Without the Exhaust Hood	12
5. Close-up Back View of the Radiant Heater Stack.	15
6. Lower View of LITA Showing the Air and Water Cooling Systems	15
7. Schematic of Radiant Heater Stack Air Cooling System and Air Supply System for the Shutter Actuating Air Cylinders	16
8. Schematic of Radiant Heater Stack Water Cooling System.	18
9. View of the Air Cylinders	24
10. View of the Shock Absorber Assemblies	27
11. View of the Sample Holder Assembly with Attached Sample and Tested Sample of Wood.	29
12. LITA Control Panel and Instrumentation.	34
13. Infrascopes Output History Plots, GIRCFF Fabric Number 17 Exposed to an Incident Heat Flux of 15.7 W/cm^2	60
14. Normalized Plots of the LITA and RITA Fabric Ignition Time Measurements.	65
15. Normalized Plots of the LITA and RITA Ignition Time Measurements of GIRCFF Fabric Number 16.	66
16. Normalized Plots of the LITA and RITA Ignition Time Measurements of GIRCFF Fabric Number 17.	67

Figure	Page
17. Normalized Plots of the LITA and RITA Ignition Time Measurements of GIRCFF Fabric Number 18. . .	68
18. Normalized Plots of the LITA and RITA Ignition Time Measurements of GIRCFF Fabric Number 20. . .	69
19. Infrascopes Output History Plots, 1/2 Inch Plywood Exposed to an Incident Heat Flux of 6.0 W/cm ²	73
20. Infrascopes Output History Plots, 1/2 Inch Plywood Exposed to an Incident Heat Flux of 6.0 W/cm ²	75
21. Normalized Plots of the LITA Wood Ignition Time Measurements	76
A.1. Top and Side Views of the Bearing Assembly for Shutter Travel and Guide.	85
A.2. Side View of the Shutter Support Assembly with Attached Shutter.	86
A.3. Top View of the Ejector Assembly.	87
B.1. Schematic of the Control Panel Electrical System (Sheet 1).	89
B.2. Schematic of the Control Panel Electrical System (Sheet 2).	90
B.3. Schematic of the LITA Power Supply System	91
B.4. Schematic of the Variac Power Supply.	92
B.5. Schematic of the Preheat Timer System	93
C.1. Infrascopes Output History Plots, GIRCFF Fabric Number 20 Exposed to an Incident Heat Flux of 15.8 W/cm ²	99
D.1. Infrascopes Output History Plots, 1/2 Inch Plywood Exposed to an Incident Heat Flux of 8.0 W/cm ²	103
E.1. Steady State, Incident Heat Flux and Preheat Time Versus Idle Heater Voltage	106

NOMENCLATURE

c	specific heat
(k/δ)	thermal conductance
$(N_{Bi})_r$	Biot number, equation (5)
$(N_{Fo})_i$	Fourier number, equation (4)
$P(B/I)$	burn injury probability given ignition
$P(B/U)$	burn injury probability given use
$P(E/U)$	exposure probability given use
$P(I/E)$	ignition probability given exposure
T_i	self-ignition temperature
T_o	environment temperature
W_o	incident radiative heat flux
x	equation (3)
z	equation (2)
δ	thickness
ρ	density
$(\rho\delta)$	mass per unit area
$\tilde{\rho}$	reflectance
σ	standard deviation of ignition time
τ_e	exposure time
$\tau_i, \langle \tau_i \rangle$	ignition time, mean ignition time
τ_p	preheat time

SUMMARY

The fire hazard of a system is quantified by the probability of fire loss given use. This fire loss probability is a function of the subprobabilities of the events that lead to a specified loss from fire. The ignition process is the first significant event of the physico-chemical processes that lead to accidental destruction by fire. The probability of ignition depends on the ratio of exposure time over mean ignition time. Thus mean ignition time characterizes the material and contributes to the fire hazard description.

Experimental and analytical research is being carried out in the Fire Hazard and Combustion Research Laboratories of the School of Mechanical Engineering, Georgia Institute of Technology, to measure and predict ignition times and frequencies as a function of material properties and heating intensities. This thesis is based on work that is part of that research effort.

The objective of this work is to design and construct an apparatus to be used for ignition time and ignition frequency measurements on thermally thick materials (furniture, interior decorations, and building materials). The apparatus is also designed to test large samples of thermally thin materials such as fabrics. An additional

objective of this work is to establish experimental techniques to facilitate acquisition of ignition time and ignition frequency data.

The Large Ignition Test Apparatus (LITA) was designed and tested. The system was characterized as follows:

- (i) uniform, time-invariant, radiative heating on samples in sizes up to 30 cm by 38 cm by 5 cm at heat fluxes between 0.25 and 16.8 watts per cm²,

- (ii) sample exposure transients below one percent of ignition time at both the start and the end of the preselected exposure interval,

- (iii) manual time exposure control, and

- (iv) remote infrared detection of ignition.

To demonstrate the feasibility of measuring ignition times, the following five fabrics were tested: two weaves of 100 percent cotton, 65 percent polyester/35 percent cotton, 50 percent polyester/50 percent cotton, and 100 percent wool. The feasibility of measuring ignition frequencies was also demonstrated using the 65 percent polyester/35 percent cotton fabric.

In addition to the fabric tests, ignition times were measured for two thermally thick materials: western fir and plywood. Samples of these materials of three thicknesses were exposed to five heating intensities.

This work has been funded by the National Science Foundation under the RANN Program (Research Applied to National Needs), grant number GI-31882.

CHAPTER I

INTRODUCTION

Relevance of Flammability Research

Among the major industrialized countries, the United States ranks highest in per capita deaths, injuries, and property damage from accidental fires. Accidental fires kill approximately 12,000 Americans each year and injure 300,000. The cost in property damage has been estimated to be in excess of \$11 billion annually [1].*

Two methods of combating this serious problem are public education and the establishment of reasonable and effective flammability standards. These standards must be rational and hence based on a foundation of fundamental research.

The first major step towards establishing such standards in this country was made by Congress in 1953 when it passed the Flammable Fabrics Act. This act had as its intent the establishment of reasonable fabric flammability criteria so as to protect the public from excessive fabric related burn injuries.

The Flammable Fabrics Act was amended in 1967 to

*The numbers in brackets refer to the references given in the Bibliography.

include additional materials such as furniture, household furnishings, and building materials. The amended act ordered the Secretary of Commerce to conduct research on the flammability of products, fabrics, and materials, conduct feasibility studies on the reduction of flammability, develop flammability test methods and offer appropriate training in the use of flammability test methods [2].

This research program was monitored during the first two years by the Government-Industry Research Committee on Fabric Flammability. This committee stated that in order to establish meaningful flammability standards it is necessary to determine the relationship between a material's behavior in the laboratory and its behavior in actual use [3]. Tribus first proposed such a relationship [4]. His proposal stated that the fire loss (or burn injury) probability is a function of the subprobabilities of the events that lead to a specified loss (or injury).

These probabilities can be classified as follows:

(i) the probability of exposure to the specified heat source given use, $P(E/U)$,

(ii) the probability of ignition given exposure to the specified heat source, $P(I/E)$,

(iii) the probability of burn injury or damage given ignition, $P(B/I)$, and

(iv) the probability of burn injury or damage given use, $P(B/U)$.

These probabilities can be expressed as:

$$P(B/U) = P(E/U) \cdot P(I/E) \cdot P(B/I) \quad (1)$$

Of particular importance is the probability of ignition given exposure to the specified heat source. The ignition process is the first significant event of the physico-chemical processes that lead to accidental injury or damage by fire. The associated probability $P(I/E)$ of ignition given exposure to a heat source during laboratory test is given by:

$$P(I/E) = (1/\sqrt{2\pi}) \int_{-\infty}^x \exp(-z^2/2) dz \quad (2)$$

The upper limit of integration is defined by:

$$x = [\tau_e / \langle \tau_i \rangle - 1] / \sigma \quad (3)$$

where τ_e is the characteristic exposure time, $\langle \tau_i \rangle$ is the mean ignition time, and σ the standard deviation of ignition time. The exposure time τ_e is the independent variable and depends on human response. The mean ignition time $\langle \tau_i \rangle$ and the standard deviation σ are evaluated from ignition frequency measurements. They both depend on material properties and exposure conditions. Thus ignition time and ignition frequency data contribute to a material's fire

hazard description.

Background of Research Program

Since 1970, an analytical and experimental program of flammability research has been conducted in the Fire Hazard and Combustion Research Laboratories of the School of Mechanical Engineering, Georgia Institute of Technology. This research has been sponsored by the National Science Foundation under the RANN Program (Research Applied to National Needs). A major part of this research has been the measurement and prediction of ignition times and ignition frequencies of thermally thin and thick materials as a function of material properties and heating intensities. This thesis is based on work that is part of that research effort.

Thesis Objectives

The objectives of this work are as follows:

- (i) to design and construct an apparatus capable of measuring ignition times and ignition frequencies of thermally thick materials,
- (ii) to verify the operation of the apparatus by measuring ignition frequencies of selected fabric samples,
- (iii) to verify the operation of the apparatus by measuring ignition times of selected fabric and wood samples, and
- (iv) to develop experimental techniques to facilitate

acquisition of this data.

The design of the apparatus is discussed in Chapter II. The operating procedures for the apparatus are presented in Chapter III. Chapter IV is a summary and discussion of the test results. Finally, Chapter V is a summary of the conclusions made and recommendations for further work.

CHAPTER II

EXPERIMENTAL APPARATUS

System Characterization

The Large Ignition Test Apparatus (LITA) was designed and built to measure ignition times and ignition frequencies of thermally thick and thin materials under radiative exposure. LITA can be characterized as follows:

(i) It provides uniform, time-invariant, radiative heating of samples in sizes up to 30 cm by 38 cm by 5 cm at heat fluxes between 0.25 and 16.8 watts per cm^2 .

(ii) Sample exposure transients are below one percent of ignition time at both the start and the end of the preselected exposure interval.

(iii) Time exposure is manually controlled.

(iv) It provides remote infrared detection of ignition.

LITA can be operated in two modes: the ignition time test mode and the ignition frequency test mode. In the ignition time test mode, the sample is exposed to the radiant heat source at fixed exposure conditions for an indefinite exposure time to obtain the material ignition time. In the ignition frequency test mode the sample is exposed to the radiant heat source at fixed exposure

conditions for a preselected interval. Several exposures are carried out at each time interval to obtain the fraction of ignitions.

There are six major sub-assemblies of LITA:

- (i) the supporting structure,
- (ii) the radiant heater stack,
- (iii) the two shutter systems,
- (iv) the sample holder and disposal system,
- (v) the instrumentation for exposure control and flame detection, and
- (vi) the exhaust system.

Figure 1 shows an overall physical view of LITA. A schematic view of the apparatus is shown in Figures 2 and 3. Details of the six sub-assemblies and their components are presented in the sections which follow.

The Supporting Structure

Eight vertical angle iron columns, six base angles, and four side braces constitute the major parts of the frame for the supporting structure. These structural components are shown in Figure 4.

Each of the eight vertical columns, P/N 22 in Figure 3, is 113 inches long and bolted to the base. The frame of the structure is composed of two inch by two inch by $3/16$ inch steel angles, and they are fastened together with $3/8$ inch diameter bolts. Most of the bracing is made from one

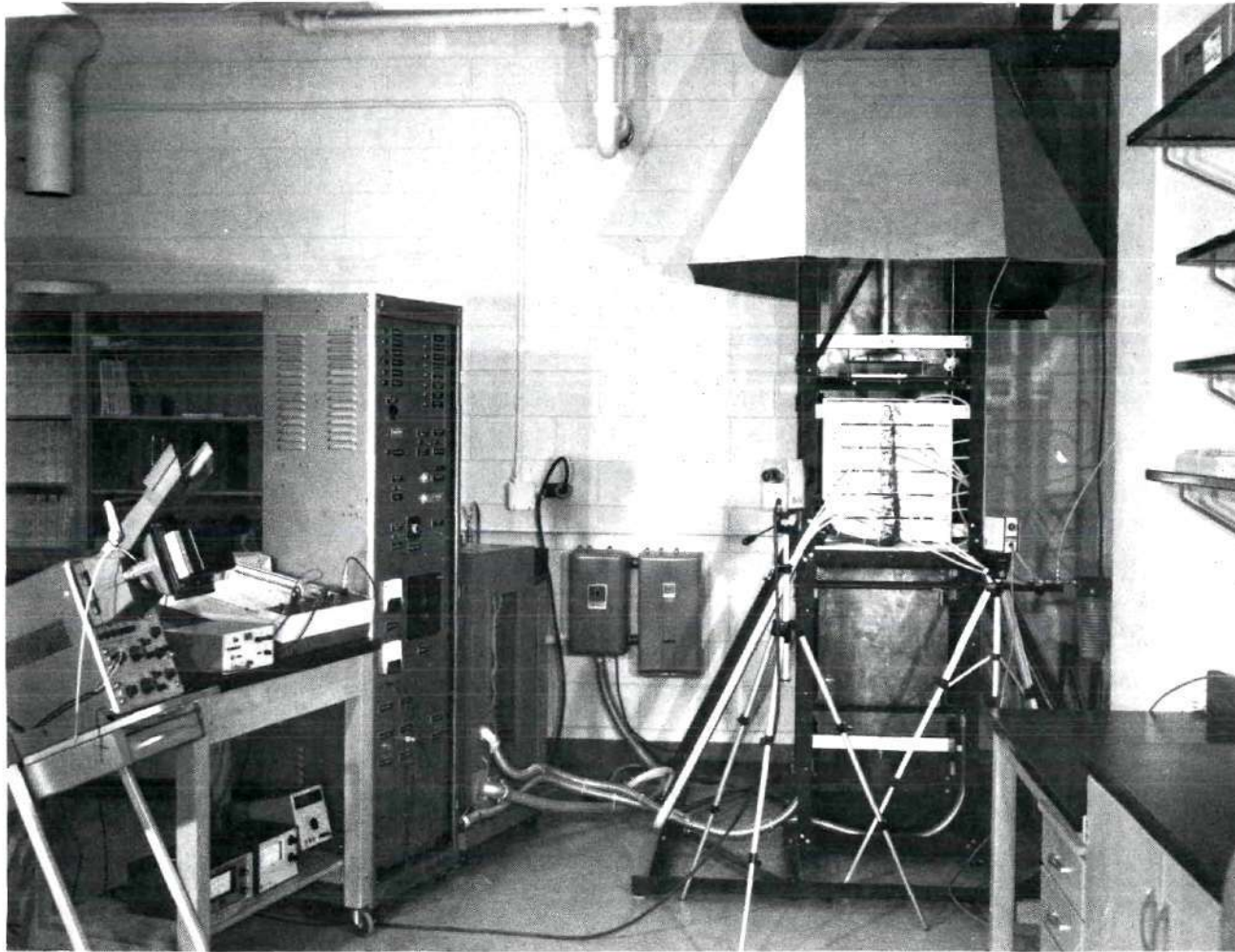


Figure 1. Overall View of the Large Ignition Test Apparatus and Associated Instrumentation

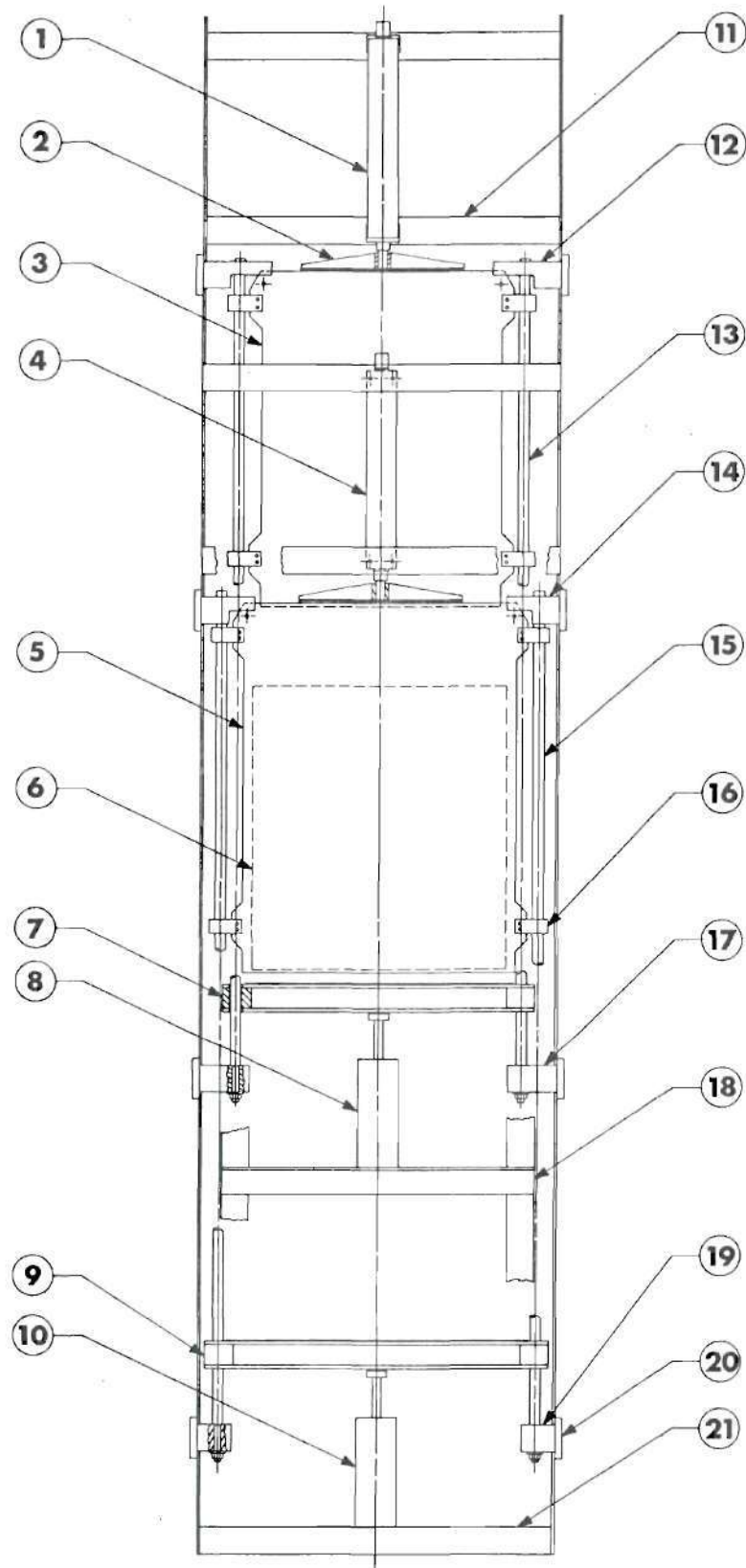


Figure 2. Assembly Drawing of LITA Without the Exhaust Hood, Front View

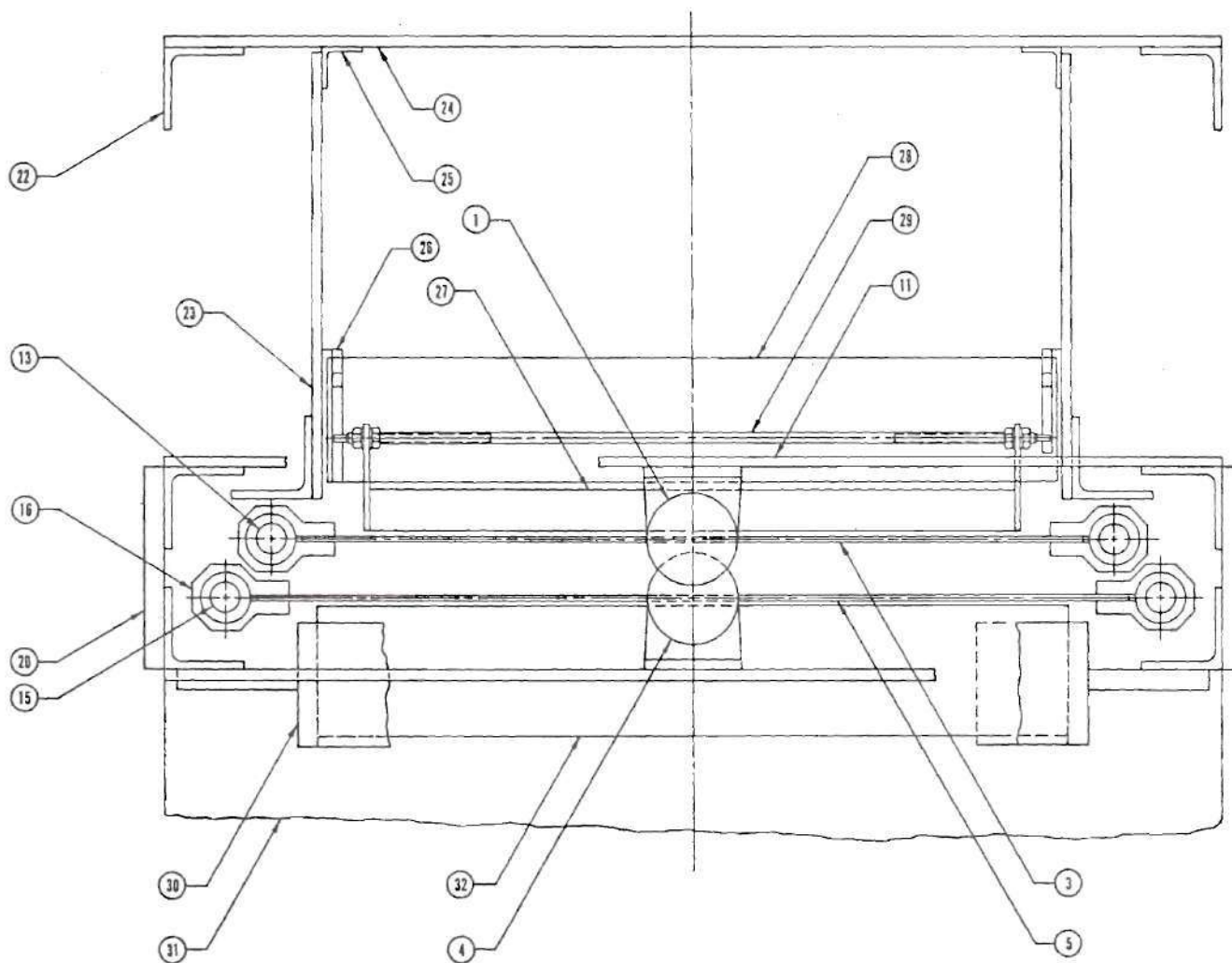


Figure 3. Assembly Drawing of LITA, Top View

Key to Figures 2 and 3

<u>P/N</u>	<u>Description</u>
1	Top Air Cylinder
2	Accelerator Bar Assembly
3	Top Shutter Plate
4	Bottom Air Cylinder
5	Bottom Shutter Plate
6	Radiant Heater Stack
7	Top Impact Bar Assembly
8	Top Shock Absorber
9	Bottom Impact Bar Assembly
10	Bottom Shock Absorber
11	Air Cylinder Support Bar
12	Top Shutter Support Assembly
13	Top Shutter Guide Rod
14	Bottom Shutter Support Assembly
15	Bottom Shutter Guide Rod
16	Bearing Assembly
17	Top Shutter Guide Rod Support
18	Top Shock Absorber Support
19	Bottom Shutter Guide Rod Support
20	Side Plate
21	Bottom Shock Absorber Support
22	Vertical Angle
23	Disposal Assembly Support Plate
24	Rear Support Plate
25	Brace Column
26	Disposal Plate
27	Sample
28	Receptacle
29	Test Specimen Support Rod
30	Heater Side Plate
31	Transite Plate
32	Radiant Heater Stack

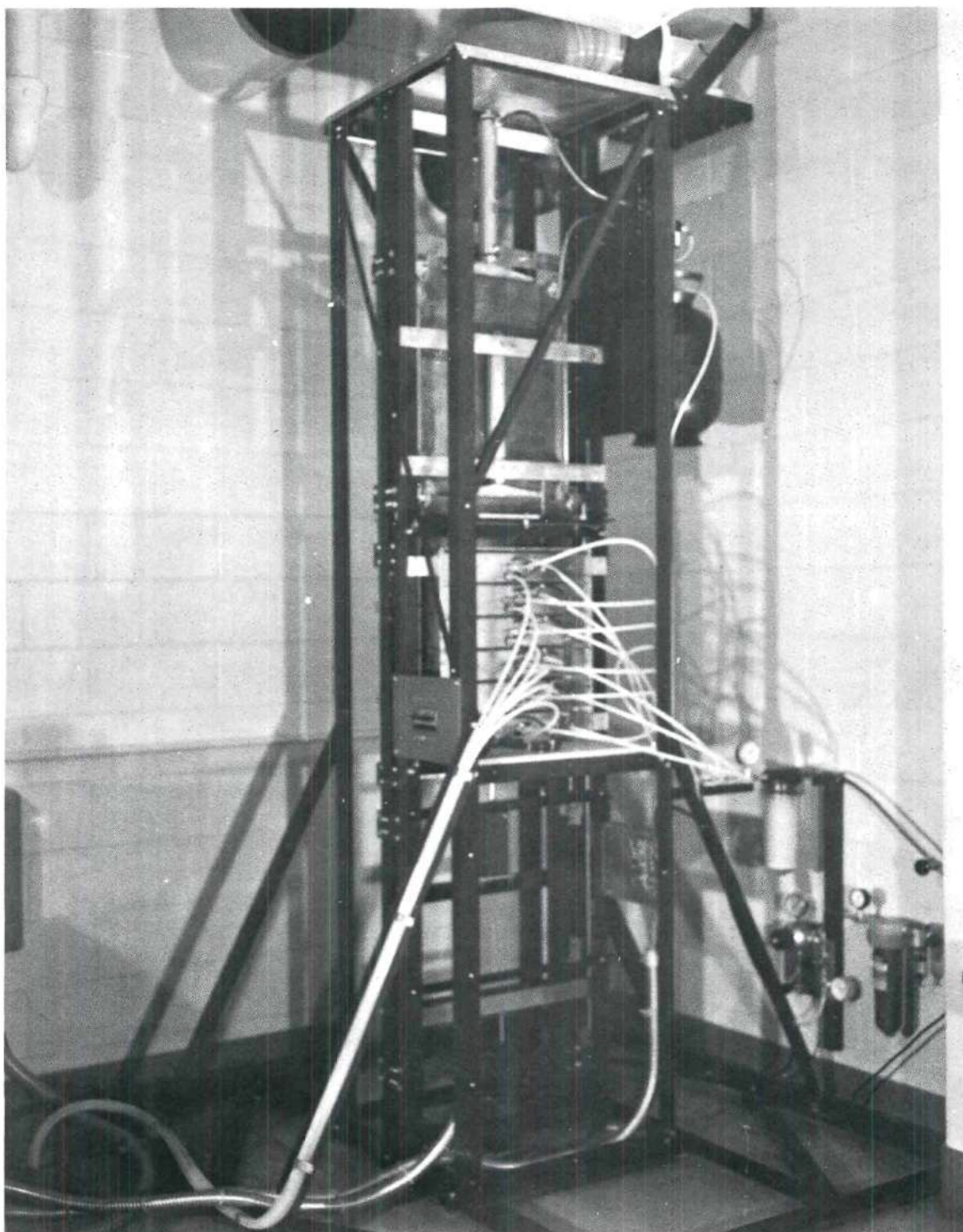


Figure 4. View of LITA Without the Exhaust Hood

inch by one inch by 1/8 inch steel angles.

The entire weight of the structure is supported by fourteen leveling screws threaded into the base. The outside dimensions of the base are 72 inches by 72 inches. The four side braces are bolted to the base and four vertical angles.

The Radiant Heater Stack and Heater Power Supply

This section describes the design of the radiant heater stack and the heater power supply. The operating procedures of this system and the other LITA sub-systems are described in detail in Chapter III.

The Radiant Heater Stack

The radiant heater stack, P/N 6 and 32 in Figures 2 and 3, consists of a heater support assembly, P/N 30, and six RI Controls radiant heaters, model number 5208-16.

Each of the RI Controls heaters, P/N 6 and 32, is rated at 40 amps at an operating voltage of 220 VAC. Each heater contains six tungsten filament, quartz envelope bulbs, type 1600 T3/1CL. The lighted portion of each bulb is sixteen inches long. The six bulbs are positioned horizontally in front of a specular aluminum reflector. Six quartz windows, each three inches by three inches are located in front of the bulbs. The total lighted area of each heater is three inches by sixteen inches.

The heater support assembly consists of two heater

side plates, one top plate, four mounting brackets, and twelve mounting plates. Each of the RI Controls heaters is attached to two of the mounting plates with two #10 screws. A 1/4 inch gap between each heater provides a partial view of the sample for flame detection.

The heater stack is supported on a 1/2 inch thick transite plate, P/N 31. This plate is mounted on two horizontal angles bolted to the structure as shown in Figure 5. To prevent any movement of the heater stack, the four mounting brackets are bolted to two of the vertical angles of the supporting structure, P/N 22, located on opposite sides of the heater stack.

The bulbs, reflector, and quartz windows of each of the RI Control heaters are air cooled. A physical view of the radiant heater air cooling system is shown in Figure 6. A schematic view of the radiant heater air cooling system is shown in Figure 7 together with the air supply system for the shutter actuating cylinders. The latter will be discussed later in this chapter. Laboratory supply air at 80 psig passes through two Sears, model 282.16008, air filters. These filters, shown in Figures 6 and 7, remove solid particles and excessive moisture from the air. After passing through the heater supply valve, the air enters the six heaters at 40 psig through separate 3/8 inch O.D. tygon tubing. This tubing is shown in Figure 5. The air enters the inlet port on the back of the heaters, passes over the

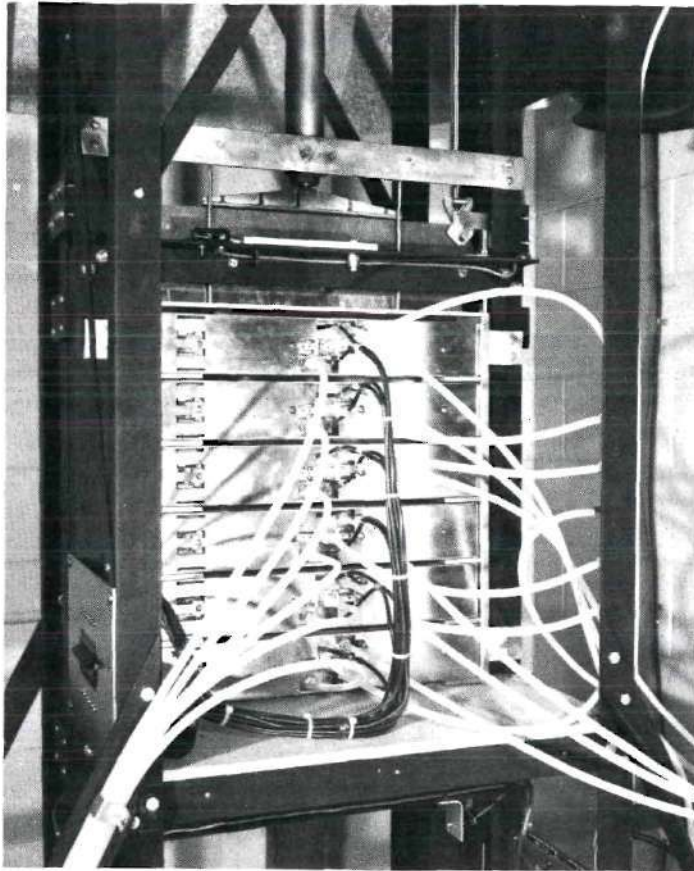


Figure 5. Close-up Back View of the Radiant Heater Stack

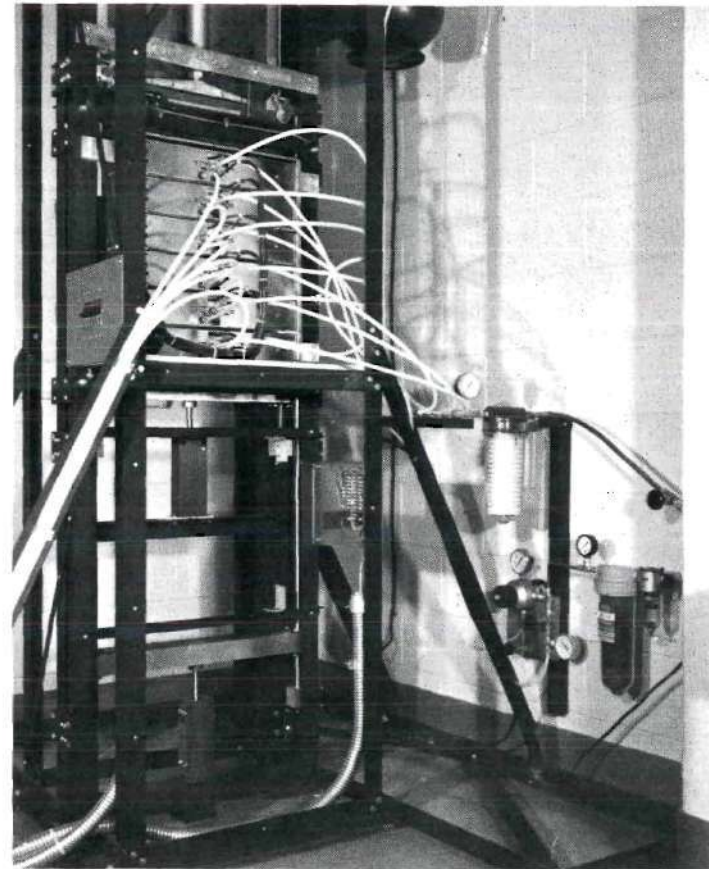


Figure 6. Lower View of LITA Showing the Air and Water Cooling Systems

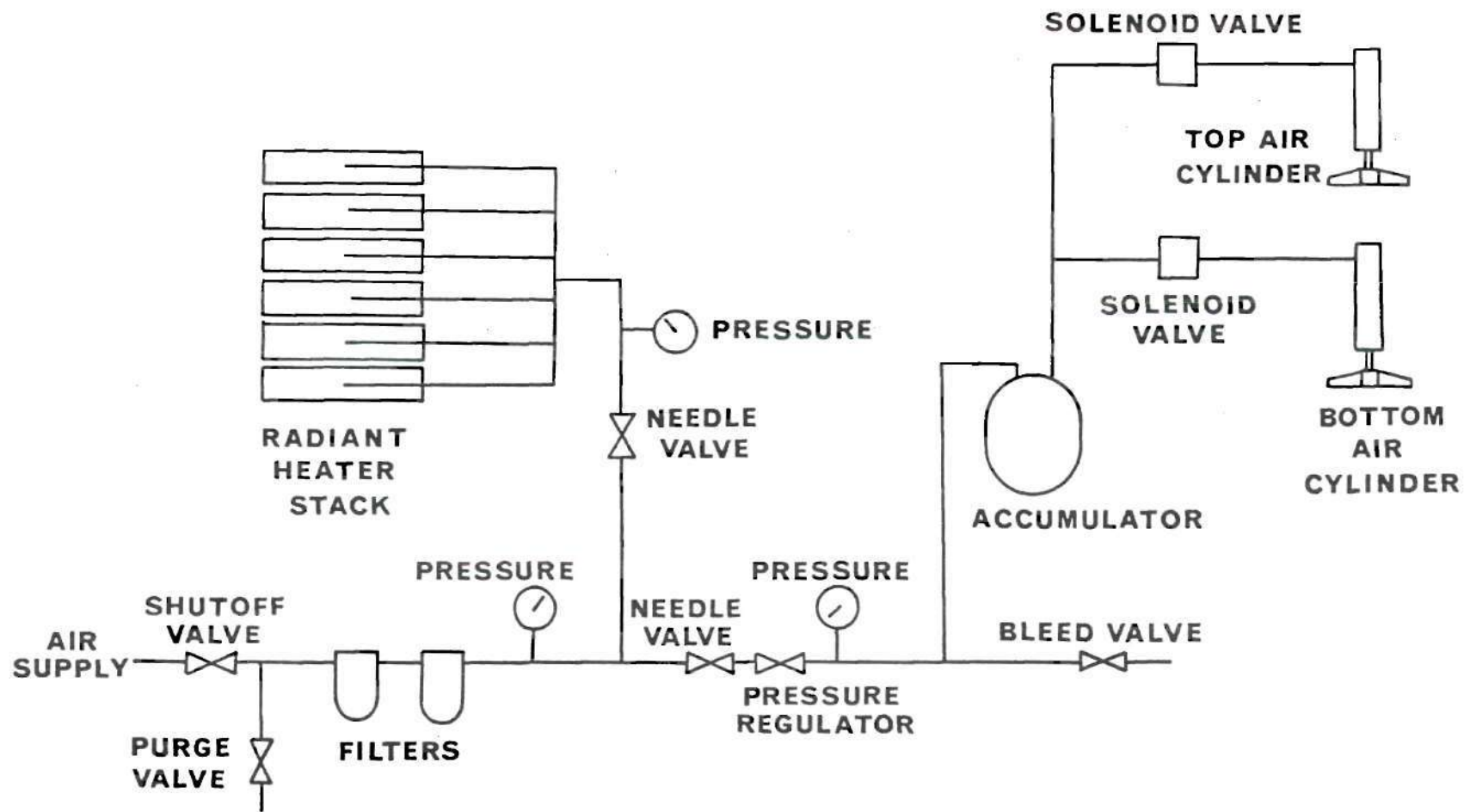


Figure 7. Schematic of Radiant Heater Stack Air Cooling System and Air Supply System for the Shutter Actuating Air Cylinders

length of the heater bulbs and then exhausts out the back of the heater case.

The case of each of the heaters is also water cooled. A schematic of the water cooling system is shown in Figure 8. Supply water passes through an AMF Cuno, model 1M1, filter. This filter removes particles larger than five microns in diameter. The water then enters the six heaters through separate 3/8 inch O.D. tygon tubing. After cooling the heater case, the water passes through another length of 3/8 inch O.D. tygon tubing and is discharged into the laboratory drain. The inlet and outlet water cooling ports are both located on the back of each of the heaters as shown in Figure 5. The total water flow rate is deduced from the pressure monitored by a mercury manometer mounted on the laboratory wall.

The Heater Power Supply

Heater and auxiliary power is provided by the high and low voltage legs of a 120 VAC, three-phase, in-house power line. Power can be turned on or off by switching two Square-D three-phase contactor assemblies, class 8502, type S, and class 8903, type Q (see Figure 1). The two contactor assemblies are remotely controlled by the main power button located on the control panel. Three red lights on each of the contactor cases indicate voltage is supplied to the contactors. The red main power light located on the control panel indicates that voltage is applied to the variac and

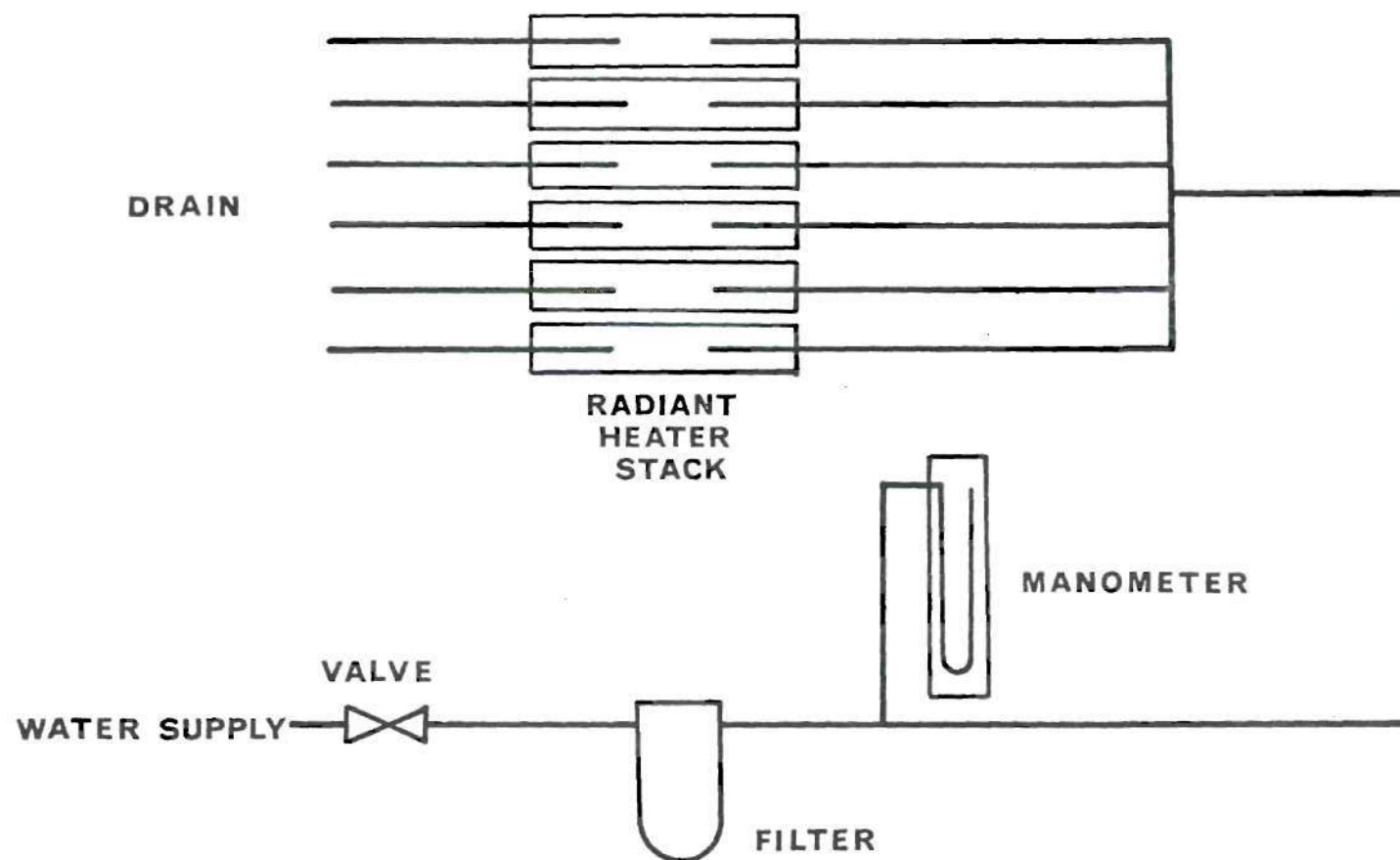


Figure 8. Schematic of Radiant Heater Stack Water Cooling System

control panel.

The power lines from the contactor boxes are enclosed in two inch diameter steel conduit and connect to the variac (see Figure 1). The variac consists of six General Electric, model 9T92Y66, variable transformers attached in parallel. The voltage supplied to the heaters is adjusted by rotating the control arm on the top of the variac. Six 45 amp power lines run from the variac to the six heaters. These lines are fused by separate 45 amp breaker switches mounted on the structure (see Figure 6). These lines are enclosed in 1-1/2 inch diameter steel conduit. Current to the heaters is monitored by a Brownell Electro, model 5N, current transformer connected to an ammeter mounted on the control panel.

Schematics of the electrical system are shown in Figures B.1-B.5.

The Shutter Systems

The two vertical shutter systems provide precise exposure time control. The two shutter systems are the top shutter system and the bottom shutter system. The bottom shutter system shields the sample from the radiant heater stack prior to test. This system prevents the sample from being preheated before the radiant heater stack reaches its steady state operating level. The top shutter system shields the sample after the preselected exposure interval. This system provides exposure time control for ignition

frequency measurements. In addition this system prevents contamination of the heater windows by the sample after termination of a test.

Each of the two shutter systems consists of:

- (i) a shutter plate,
- (ii) four bearing assemblies,
- (iii) two vertical shutter guide rods,
- (iv) an air cylinder and attached accelerator bar assembly,
- (v) a solenoid valve and connecting tubing,
- (vi) two shutter support assemblies,
- (vii) two rod support bars, and
- (viii) an impact bar assembly and an adjustable shock absorber.

In addition, air for both the top and bottom shutter systems is provided by a single accumulator. Locations of these components are shown in Figures 2 and 3.

Operation of the shutter systems is briefly described as follows. Prior to exposure, the sample is shielded by the bottom shutter, P/N 5, which is located 1/8 inch in front of the heater stack. After actuation of the bottom air cylinder, P/N 4, the bottom shutter travels below the sample heating area and is stopped by the bottom shock absorber, P/N 10. After a specified exposure period the top air cylinder, P/N 1, is actuated. The top shutter, P/N 3, then travels downward and is stopped by the top shock absorber,

P/N 8. In its rest position, the top shutter shields the sample, P/N 27, from the heater stack, P/N 6 and 32. Additional details of this operation are given in the remainder of this section.

Both shutter plates are made from 1/8 inch thick cold-rolled copper plates. Copper was selected to provide the capability of soldering copper tubing for cooling. The tubing was not added since the necessary preheat period proved to be shorter than originally anticipated.

The top shutter plate is 19.36 inches wide and 24.67 inches long and weighs approximately sixteen pounds. The bottom shutter plate is 21.64 inches wide and 27.20 inches long and weighs approximately 18 pounds.

As shown in Figure 2, attached to each shutter are four bearing assemblies, P/N 16. Each bearing assembly consists of a bearing housing and a Thompson Series A linear ball bushing (model A122026). Two retainer rings hold the ball bushing in the housing. Each bearing assembly is mounted onto the shutter with two #10 screws. One side of the shutter has four screw access slots to allow for thermal expansion of the shutter. The bearing assembly is shown in Figure A.1 in the Appendix.

Each shutter assembly slides on two 3/4 inch diameter, 1040 steel rods. Both rods are case hardened. The top shutter guide rods, P/N 13, are 69 inches long, and the bottom shutter guide rods, P/N 15, are 67 inches long.

These rods are manufactured by Thompson Industries, Incorporated.

The rods are supported at the bottom by two aluminum rod supports and at the top by two shutter support assemblies as shown in Figure 2. Each of these parts is supported by separate aluminum side plates, P/N 20, which are bolted to the structure.

Prior to actuation of the air cylinder, each shutter is supported by two shutter support assemblies located at the top and on opposite sides of the shutter. Each spring support assembly cradles a 1/4 inch diameter steel roll pin that is press-fit through the shutter plate. The roll pin is shown in Figure A.2 in the Appendix. When the air cylinder is actuated the shutter roll pin is forced past the shutter support assembly allowing the shutter to accelerate downwards. A force of approximately five pounds is required to release the shutter.

The shutter support assembly, shown in Figure A.2 in the Appendix, consists of an aluminum shutter support bar, four aluminum pivot arms, a supporting bolt, and two PIC Corporation extension springs, number AZ-84. A 1/4 inch screw and nut attached to two of the pivot arms maintains a small gap between the pivot arms when the shutter roll pin is not in place. This design feature enables the operator to load the shutter in the shutter support assembly by lifting the shutter at the bottom edge until both roll pins

are locked into place.

Both shutters are accelerated by Parker Hannifin air cylinders, model number 2PR16X6. The top air cylinder, P/N 1, and the bottom air cylinder, P/N 4, are shown in Figures 2 and 9. Both air cylinders have two inch bores and six inch strokes. After actuation, an internal spring returns the air cylinder piston to its original position.

Each of the air cylinders is bolted to the two air cylinder support bars, P/N 11. These bars are mounted horizontally on the structure columns. The accelerator bar assembly, P/N 2, is threaded onto the end of the air cylinder piston rod. The accelerator bar assembly consists of an aluminum bar and a 1/4 inch thick neoprene pad. The neoprene pad provides uniform contact of the assembly with the shutter.

The accelerator bar assembly slides against two vertical guide rods. These rods are made from 1/8 inch diameter aluminum rod. The guide rods prevent the accelerator bar assembly and air cylinder piston from rotating during actuation.

Air is supplied from the accumulator to two Modernair solenoid actuated poppet valves, model number 5231-2633-03, as shown in Figure 7. Each solenoid valve is actuated by turning on its respective solenoid valve toggle switch located on the control panel. A red light above each toggle switch indicates that the switch is turned on. For safety

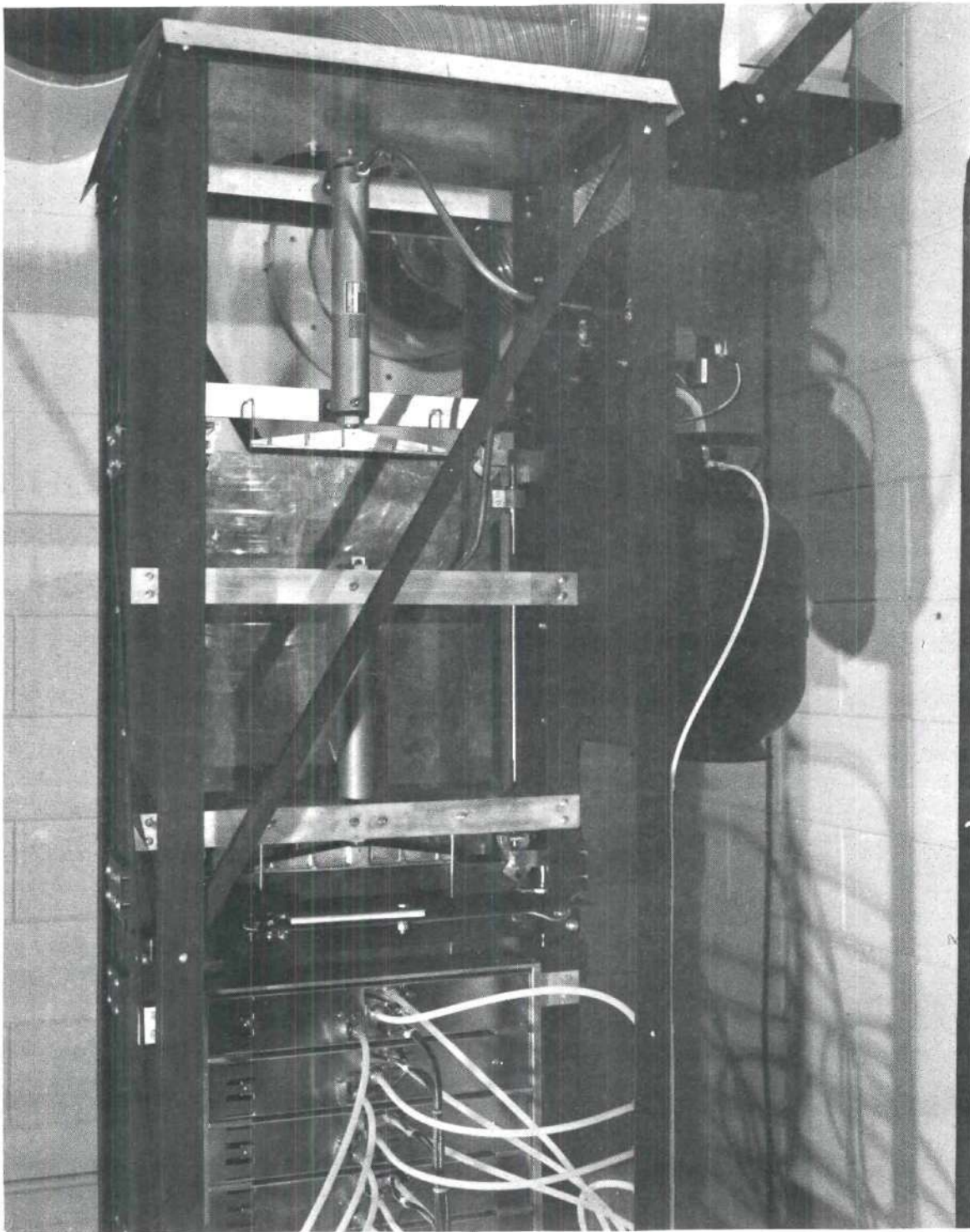


Figure 9. View of the Air Cylinders

purposes, the arming switch located on the control panel must be turned on for either solenoid valve to be actuated. A red light above the arming switch indicates that the system is armed. As an additional safety precaution, two amber lights located on the control panel indicate that the respective solenoid valve toggle switches are turned off prior to arming the system. When either solenoid valve is actuated, air flows from the valve to its respective air cylinder. One-half inch O.D. tygon tubing is routed between the accumulator and the solenoid valves, and 1/2 inch O.D. copper tubing was routed between the solenoid valves and the air cylinders. The total tubing lengths between the accumulator and both air cylinders were sized the same to insure equal pressure drops.

An Air Products, model E11-1-N5108, air regulator can supply air to the accumulator at pressures up to 60 psig. The accumulator is a converted Freon-12 tank. The tank is mounted on a plywood board bolted to the side of the structure midway between the top and bottom air cylinders. The two solenoid valves are also mounted on the plywood board, above the accumulator.

After actuation the bottom shutter, which exposes the sample to the radiant heaters, travels 57 inches before being decelerated by the bottom shock absorber. The length of travel of the top shutter is 51 inches.

The top impact bar assembly, P/N 7, and the bottom

impact bar assembly, P/N 9, are shown in Figure 2. Each impact bar assembly consists of:

- (i) an aluminum impact bar,
- (ii) a neoprene pad,
- (iii) two nylon bushings, and
- (iv) four bushing retainer plates.

The neoprene pad is 1/4 inch thick. It is located on top of the impact bar and prevents deformation of the shutter. The two nylon bushings are mounted in opposite ends of the impact bar. Each bushing is secured at the top and bottom with two bushing retainer plates. These plates are attached to the impact bar with four #10 screws.

Each nylon bushing slides on one of the four shutter guide rods as shown in Figure 2. The top impact bar assembly, P/N 7, rests on the top shock absorber, P/N 8, and the bottom impact assembly, P/N 9, rests on the bottom shock absorber, P/N 10, as shown in Figure 2. Both shock absorbers are Efdyn Corporation adjustable hydraulic shock absorbers, model ASB-1-3PS99. After impact with its respective impact bar assembly, each shutter linearly decelerates over a distance of three inches. The resisting force of the shock absorber can be adjusted by turning the adjustment screw at the bottom of the shock absorbers. A physical view of both shock absorbers is shown in Figure 10.

As a safety precaution between tests, the top shutter can be raised above the heater area and supported by

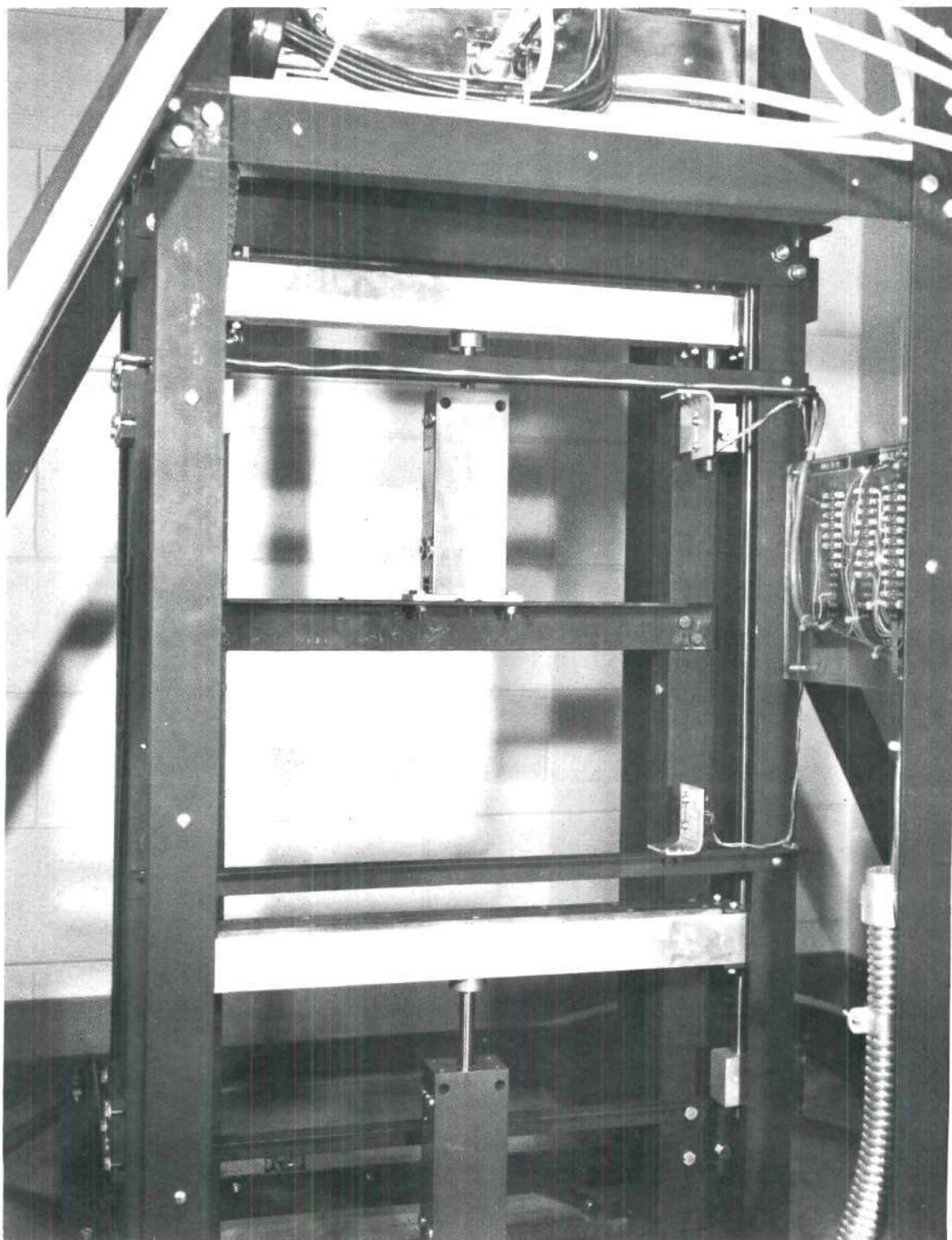


Figure 10. View of the Shock Absorber Assemblies

an aluminum mechanical block. The block is supported by two one inch by one inch by 1/8 inch angles mounted on the structure. The block pivots about a 1/4 inch diameter bolt that is positioned through the block and the support angle. To insure that the block is not in the path of the shutter during test, the block is pivoted against the trigger arm of a micro-switch. When the block is pinned in this position, an amber light on the control panel indicates that the block is retracted.

The Sample Holder Assembly and Disposal System

LITA has been designed to accomodate both thermally thin materials (fabrics) as well as thermally thick material up to five inches in thickness. To accurately position these variable size samples in front of the heater stack, a special sample holder assembly was incorporated into the design of LITA. In addition, the sample holder assembly was designed with the capability to dispose the burning sample into a receptacle partially filled with water.

The sample holder assembly, P/N 29 in Figure 3, also shown in Figure 11, can directly accommodate wood samples of the following sizes: thicknesses from 1/8 inch to two inches and widths up to sixteen inches. Larger widths can be accommodated by introducing some minor modifications on the sample holder assembly. The wood sample is held between

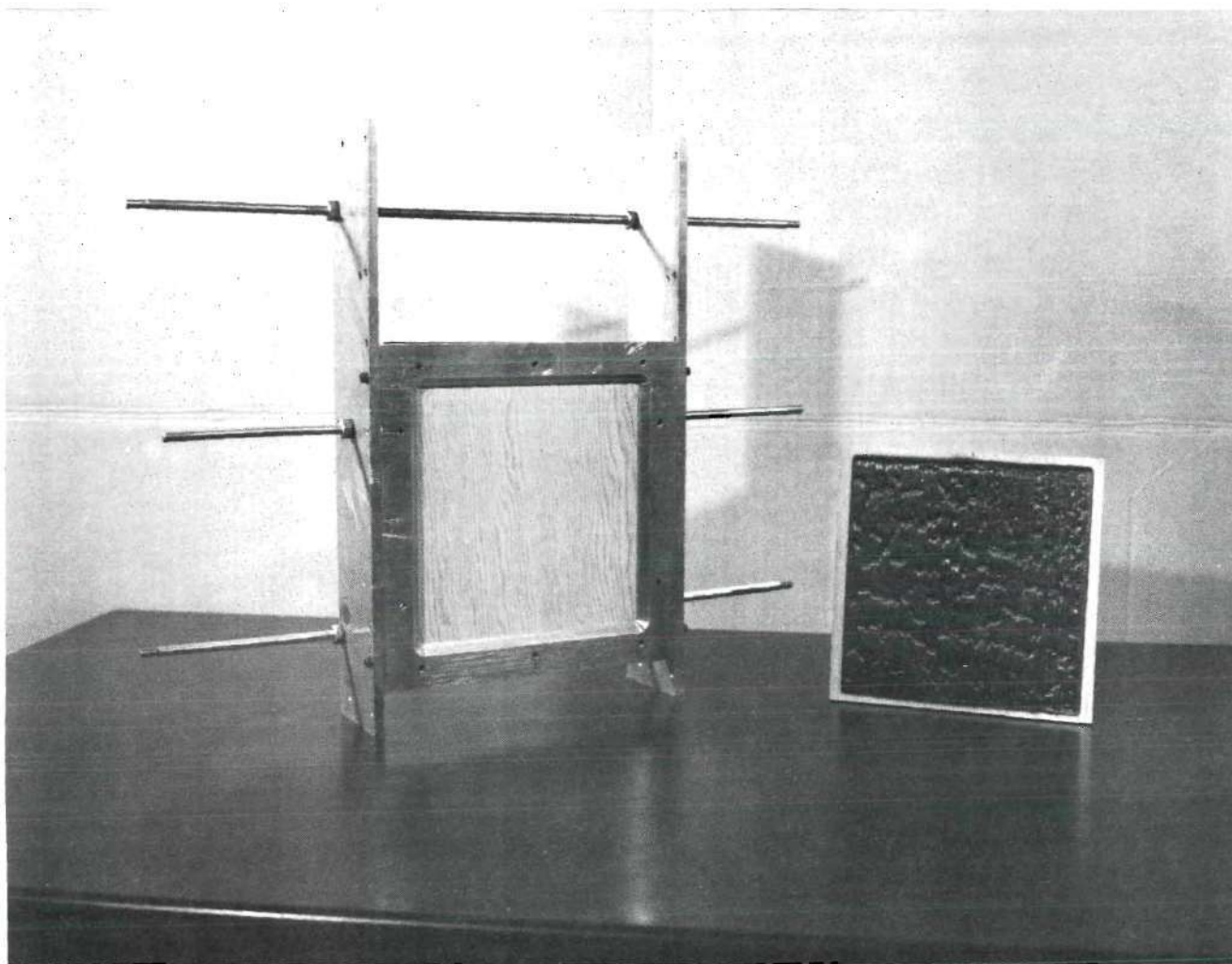


Figure 11. View of the Sample Holder Assembly with Attached Sample and Tested Sample of Wood

two parallel 1/4 inch thick aluminum sample holder plates. These plates are fastened together with three 1/4 inch O.D. threaded aluminum rods. The three rods are secured to the two sample holder plates with twelve nuts and lock washers. Additional sample support is provided by 5/8 inch long fastening pins. These fastening pins thread into the sample holder plates and pierce the sample with their conical tips.

To accommodate six inch by six inch samples (fabrics and wood), the sample holder was designed. The latter consists of an eight inch by eight inch frame with a six inch by six inch center. Fabric samples are secured with four aluminum bars that are fastened with ten #8 screws to the back of the frame. Wood samples are similarly attached with two bars and four #8 screws.

The ends of two of the three aluminum threaded rods were turned to a nominal diameter of .187 inch. The ends of these rods slide in four horizontal grooves machined in the two disposal plates, P/N 26. The plates are bolted to two vertical angles of the supporting structure. The angles are 67 inches long and are located on opposite sides of the heating area.

The force required to accelerate the sample holder assembly is provided by four PIC Corporation compression springs (number AY-70). These springs are located in two holes machined in each of the two disposal plates. A nylon tip attached to each spring pushes the end of the rod. The

compression force of each spring can be adjusted by advancing a set screw threaded into the disposal plate.

The sample holder assembly is prevented from moving prior to ignition by four ejector assemblies which were incorporated into the design of LITA. Each ejector assembly consists of:

- (i) an ejector block pin,
- (ii) a compression spring,
- (iii) a spring support,
- (iv) a Dormeyer solenoid, model number C9-519-A-14,
and
- (v) a solenoid mounting plate.

Two ejector assemblies are located on each side of the sample heating area. A view of the ejector assembly is shown in Figure A.3 in the Appendix.

The operation of the ejector assembly is as follows. Prior to actuation of the solenoid, the end of the ejector block pin is located in the path of the sample holder assembly rod. In this position, a positive force is applied to the block pin by the one inch diameter compression spring. After actuation of the solenoid, the ejector block pin retracts. The sample holder assembly is then allowed to travel away from the heating area.

The ejector assembly solenoids can be actuated by turning on either of two toggle switches. One of these switches is located on the control panel and the other on the

structure near the disposal plate. To insure proper operation of the ejector assemblies during an actual test, an amber light on the control panel indicates that the disposal toggle switches are turned off prior to a test. In addition, a red light above the ejector toggle switch on the control panel indicates the ejector assemblies are retracted.

After actuation of the ejector assemblies, the sample holder rods travel $3/4$ inch in the horizontal grooves in the direction away from the heaters. The rods then slide down a thirteen inch vertical groove machined in the disposal plates. The sample holder assembly then drops into the receptacle. The receptacle is partially filled with water to extinguish the flames.

The receptacle, P/N 28, in Figure 3 is 44 inches high. The length and width of the receptacle are $18\text{-}1/2$ and $3\text{-}3/4$ inches, respectively. The receptacle is constructed from 24 gauge galvanized steel sheet metal. The three sections of the receptacle are fastened together with steel pop rivets. The seams of the receptacle are sealed with silicon rubber. The inside of the receptacle is painted to prevent corrosion.

Manual drainage control is provided by a $1/2$ inch diameter drain port located near the bottom of the receptacle. A $3/4$ inch diameter neoprene hose and valve connect the drain port to the laboratory drain.

Instrumentation

LITA's instrumentation performs the following tasks:

- (i) It controls heater power.
- (ii) It monitors the air and water cooling systems.
- (iii) It controls the air system for shutter actuation.
- (iv) It controls exposure time.
- (v) It detects ignition of the sample.

Figure 1 shows this instrumentation together with LITA. Figure 12 is a close-up view of some of the recording and control instruments. The instrumentation which performs the first three of these tasks has been discussed previously in this chapter. This section describes the instrumentation for exposure control and the instrumentation for flame detection. This section also lists the instruments mounted on the control panel.

Instrumentation for Exposure Control

The instrumentation for exposure control monitors shutter velocities, exposure time, and heater power. Measurements of shutter velocities provide a check on exposure transients.

The bottom shutter velocity is monitored by two Robertshaw, model BRD2-LW-228-1S, micro-switches. The upper micro-switch is positioned so that when the top edge of the shutter is in line with the top of heater number two the trigger arm of the micro-switch is deflected. (The heaters

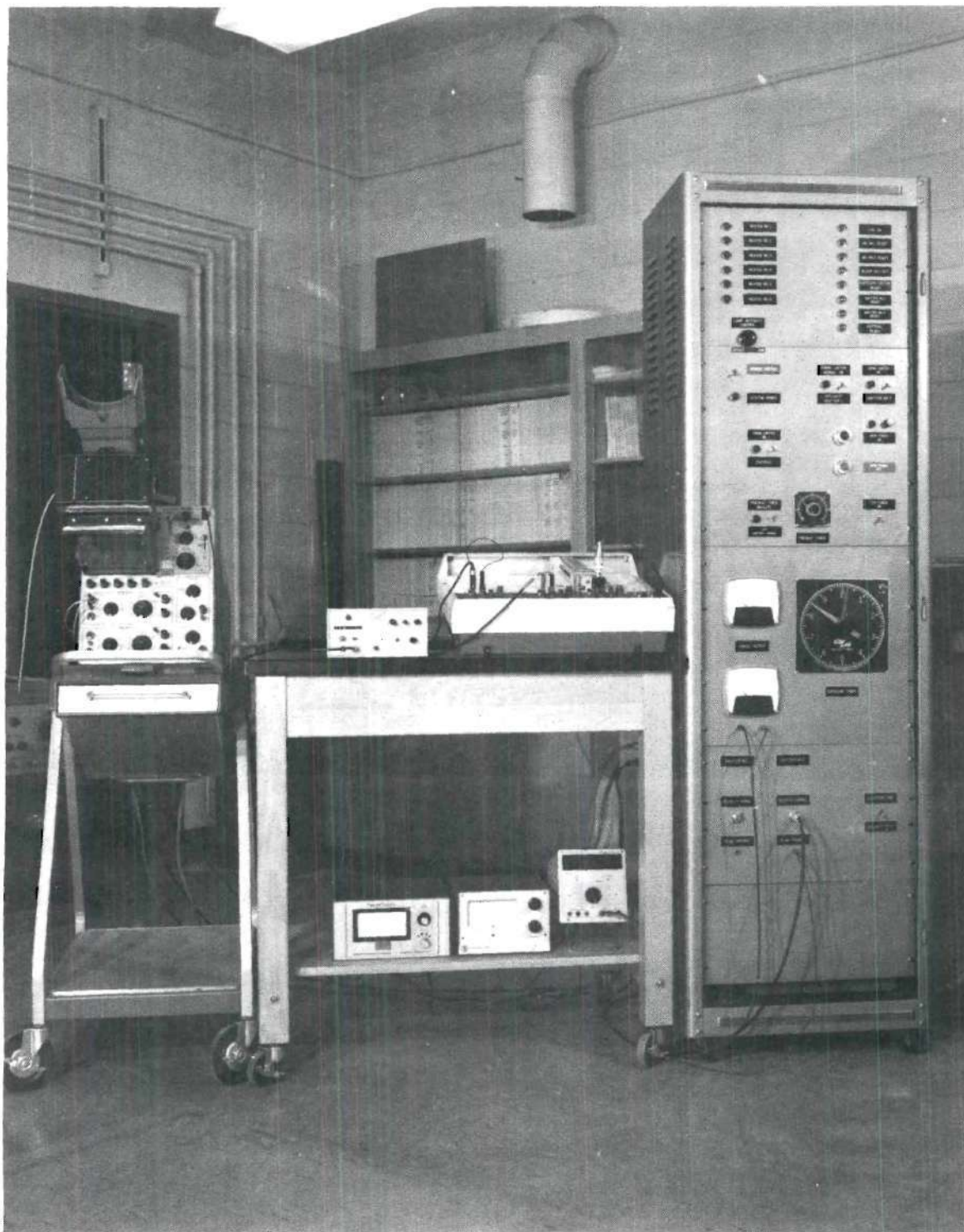


Figure 12. LITA Control Panel and Instrumentation

are numbered sequentially from the top.) With the test mode toggle switch in the velocity position, a +12 VDC signal then deflects the trace of a Tektronix, model 502A, dual-beam oscilloscope. When the arm of the lower micro-switch is deflected, the input to the oscilloscope returns to zero potential, and the trace is again deflected. This second deflection occurs when the top of the shutter is even with the top of heater number six.

The trace of the oscilloscope is recorded by a Polaroid camera, model C-27. Knowing the distance between the two micro-switches (fifteen inches) the average velocity of the bottom shutter can be calculated.

The velocity of the top shutter is similarly monitored by two Robertshaw, model BRD2-LW-228-1S, micro-switches. The upper micro-switch is located such that the arm is deflected when the bottom edge of the shutter is even with the top of heater number two. The bottom micro-switch is deflected when the shutter hits the top impact bar. The shutter travel monitored measures nineteen inches. The signals produced by the two micro-switches are identical to those of the bottom shutter micro-switches. These signals are also inputted into the Tektronix oscilloscope and recorded by the Polaroid camera.

For either shutter velocity test, the oscilloscope can be triggered by the pulse that actuates either solenoid valve or by the internal change in dc voltage when the upper

micro-switch is triggered.

In addition to shutter velocities, total exposure time can be monitored. For the ignition time tests, the exposure time is indefinite. This time is monitored by the flame detection system which is described in detail in the next section of this chapter.

For the ignition frequency tests, exposure time is monitored by a Fisher model 6-66-40 micro-timer. With the test mode toggle switch in the exposure time position, the micro-timer is started when the bottom shutter deflects the arm of the lower micro-switch. After the preselected exposure period, the top shutter solenoid valve is actuated by turning on the top shutter solenoid valve toggle switch. When the lower top shutter micro-switch is deflected (corresponding to impact of the top shutter with the impact bar assembly) the micro-timer is stopped to record an interval of exposure time.

In addition to exposure times and transients, heater power is monitored. Heater power is correlated to idle heater voltage as discussed in Chapter IV. This voltage is measured by a Honeywell model 333R digital voltmeter located next to the control panel (see Figure 12). Total heater current is also monitored by an ammeter mounted on the control panel.

The six green indicator lights on the control panel also provide a check that power is supplied to each of the

heaters. The intensity of these lights can be adjusted by turning the brightness control knob located on the control panel. This design feature prevents bulb burn-out when the variac voltage is at maximum value.

Instrumentation for Flame Detection

The flame detection system consists of a Barnes Engineering Mark 1 and a Barnes Engineering Temptron infra-scopes. The Mark 1 infrascopes is positioned approximately three feet behind the heater stack. The Temptron infrascopes is positioned approximately four feet behind the heaters. Both cameras are aimed through one of the 1/4 inch gaps between the heaters and focused on the sample.

The signals from the infrascopes are inputted into the two Y axis channels of a Hewlett-Packard, model 7046A, X-Y plotter. A Disa, model 52B01, sweep drive unit produces the time base for the X axis of the plotter.

The Control Panel

The control panel has been designed to provide central control and monitoring of the major functions of LITA. Most of the instruments mounted on the control panel have been discussed in the preceding sections of this chapter in association with the various sub-assemblies. However, for conciseness all of the control panel instruments are listed in this section.

The control panel is composed of five aluminum panels mounted end to end as shown in Figure 12. The top panel

contains the system indicator lights. On the left side of this panel are the six heater power indicator lights and lamp brightness control knob. On the right side of this panel are:

- (i) the fan power light,
- (ii) the two micro-switch ready lights,
- (iii) the mechanical block indicator light,
- (iv) the exposure switch ready light,
- (v) the two solenoid valve toggle switch ready lights, and
- (vi) the disposal toggle switch ready light.

When all of these indicator lights are lit, the system is ready for test.

The second panel from the top contains the following control switches and lights:

- (i) the arming switch and indicator light,
- (ii) the two solenoid toggle switches and their respective indicator lights,
- (iii) the disposal toggle switch and indicator light,
- (iv) the main power button and main power light,
- (v) the fan power toggle switch,
- (vi) the preheat timer, and
- (vii) the preheat timer test mode toggle switch and auto mode indicator light.

The preheat timer is a Haydon at Torrington, model BN4222-004E, 30 second timer. The preheat time of the heater stack can be

controlled by manually adjusting this timer to any desired interval up to 30 seconds. With the preheat timer test mode toggle switch in the auto position, the heaters are automatically preheated when the main power button is turned on. After the preselected preheat time interval, the bottom shutter solenoid valve automatically actuates. The bottom air cylinder piston then moves downward accelerating the bottom shutter. The period of time this piston is extended is controlled by a Potter and Brumfield, model CHB-38-70003, delay timer. The delay timer is manually adjusted so that after a two second period power to the bottom shutter solenoid valve is cut off and the piston retracts. This design feature prevents the neoprene pad of the accelerator bar assembly from over heating during a test. The delay timer is located inside the control panel cabinet behind the second panel.

The third panel contains the exposure timer, ammeter, and voltmeter for exposure monitor.

The output jacks for the bottom shutter velocity test and the top shutter velocity test are mounted on the fourth panel. The fourth panel also contains the test mode toggle switch.

The fifth panel provides the capability of adding additional instrumentation for future modifications.

The Exhaust System

The final sub-system of LITA is the exhaust system. The exhaust system consists of a collecting hood, an exhaust fan, and two connecting hoses. The exhaust system is designed to effectively collect and exhaust smoke and combustion gases to an outside vent.

The exhaust hood, shown in Figure 1, is attached with four 1/4 inch diameter bolts at the top of the supporting structure. Sandwiched between the hood and the structure are two 1/4 inch thick neoprene strips. These strips dampen hood vibration and provide a firm seat for the hood. The hood is constructed from five sections of 24 gauge, galvanized steel sheet metal. The hood sections are fastened together with #6 sheet metal screws.

An eight inch diameter hole is located directly above the sample area. Smoke and combustion gases pass through this hole into an eight inch diameter flexible plastic hose. One end of this hose is attached to a steel flange ring bolted on the top of the hood. The other end of the hose connects to the inlet of a 3/4 horsepower centrifugal fan mounted on the laboratory wall one foot above the top of the hood.

Another eight inch diameter plastic hose connects the outlet of the fan to the inlet of the laboratory exhaust duct.

The exhaust fan operates on 120 VAC. Power to the fan

is controlled by a toggle switch located on the control panel. An amber light on the control panel indicates the fan is operating.

CHAPTER III

EXPERIMENTAL PROCEDURE

This chapter describes the experimental procedure used to measure (i) the heat flux and total current of the radiant heater stack, and (ii) the top and bottom shutter velocities. The procedures for preparing the fabric and wood samples for test are also included in this chapter. Finally, the procedures used to determine the ignition times and frequencies of fabric and wood samples are presented.

Measurement of the Heat Flux of the Radiant Heater Stack

Before measuring ignition times and frequencies of fabric and wood samples, the heat flux of the radiant heater stack was measured. The purpose of these measurements was to:

- (i) determine the area of uniform heat flux,
- (ii) correlate idle heater voltage with steady state incident heat flux, and
- (iii) correlate idle heater voltage with the preheat time required by the heaters to reach steady state operation.

To determine the area of uniform heat flux, the steady state incident heat flux was measured at 35 locations with 204 VAC idle heater voltage. These 35 locations were spaced evenly over the entire heating area. Twenty-four of these

locations corresponded to positions directly in front of the heater bulbs. The other 11 locations corresponded to positions between adjacent heaters. The steady state incident heat flux was also measured at 18 locations at an idle heater voltage of 105 VAC. Thirteen of these locations corresponded to positions spaced evenly in front of the heater bulbs of the top three heaters. The other five locations corresponded to positions between the top three heaters. At both voltages, the heat flux was measured with a Hy-Cal, model C-1301-A-15-072, heat flux sensor. This sensor was secured in an asbestos plate mounted in front of the heater stack. The position of the sensor was adjusted to coincide within 1/16 inch of the sample plane facing the heaters. The distance between the sample plane and each of the heater windows is 5.1 cm (two inches). During operation, the sensor was water cooled. Cooling water was supplied from the laboratory spigot through 3/8 inch diameter tygon tubing connected to 1/8 inch diameter copper tubing. The cooling water was then routed into the laboratory drain through similar lengths of tubing.

Prior to test, cooling air and water were supplied to the heaters as discussed in the sixth section of this chapter. Cooling water for the heat flux sensor was turned on and adjusted to 70°F. The top shutter was locked into place. Power was supplied to the heaters in the same manner as described in the sixth section of this chapter with the

following exceptions: the preheat timer was not used, and the shutters were not actuated. The output of the heat flux sensor was recorded by a Leeds and Northrup Speedomax Recorder. The maximum output of the sensor was correlated to the steady state incident heat flux as calculated from the sensor calibration curve supplied by the manufacturer. The results of these tests are reported in Chapter IV.

The Hy-Cal heat flux sensor and Speedomax Recorder were used in a similar manner to correlate idle heater voltage with (i) steady state incident heat flux and (ii) the preheat time required by the heaters to reach steady state operation. The heat flux sensor was positioned in the area of uniform heat flux as determined above. The output of the sensor was recorded by the Speedomax Recorder at idle heater voltages between 50 VAC and 200 VAC in increments of 10 VAC. For each test the maximum sensor output was correlated to the steady state incident heat flux for the given idle heater voltage. In addition, the time taken by the heaters to reach this steady state heat flux level was recorded as the characteristic preheat time for the particular idle heater voltage. These results are presented in Chapter IV.

Measurement of the Heater Current

The total current of the radiant heater stack was measured for future checks on the heater performance.

Heater current was measured during each of the steady state incident heat flux measurement tests as described in the previous section of this chapter. Total current was monitored by the ammeter mounted on the control panel. These measurements are correlated with idle heater voltage in the next chapter.

Measurement of Shutter Velocities

The velocities of the top and bottom shutters were measured to provide a check on exposure transients at the start and end of the exposure interval. These tests were conducted prior to measuring ignition times and frequencies of the fabric and wood samples.

The velocity of the bottom shutter was monitored by the two bottom shutter micro-switches. As discussed in Chapter II, the trace of the oscilloscope was deflected when the arm of each micro-switch was deflected by the bottom edge of the shutter. Consequently the velocity measured was the average velocity of the shutter between the times its top edge was even with the top of heater number two and the top of heater number six. The shutter reached the first position after traveling $8\frac{5}{8}$ inches.

The velocity of the top shutter was similarly monitored by the two top shutter micro-switches as described in Chapter II. The velocity measured was the average velocity of the shutter between the time its bottom edge was even with heater

number two and the time it contacted the impact bar assembly. The top shutter traveled 8-5/8 inches before contacting the first of the two micro-switches.

For each shutter velocity measurement, the shutter was locked into its respective shutter support assemblies. The accumulator was filled to a pressure of 30 psig by adjusting the pressure regulator. Power was applied to the control panel as discussed in the sixth section of this chapter. Power was applied to the oscilloscope, and the film of the Polaroid camera was exposed to the oscilloscope screen. With the test mode toggle switch in the velocity position and the arming switch turned on, the respective shutter solenoid valve toggle switch was turned on. The shutter solenoid valve then actuated, and the shutter accelerated downward. Knowing the sweep rate of the oscilloscope, the average shutter velocity was calculated from the oscilloscope trace recorded by the camera. The results of the two shutter velocity tests are presented in Chapter IV.

Fabric Sample Preparation

In order to verify the feasibility of measuring ignition times, the following five fabrics were tested: two weaves of 100 percent cotton, a 65 percent polyester/35 percent cotton, a 50 percent polyester/50 percent cotton, and a 100 percent wool. The feasibility of measuring ignition frequencies was also demonstrated using the 65

percent polyester/35 percent cotton fabric. The procedure used to prepare fabric samples for the ignition time and ignition frequency tests are the same. The remainder of this section is a discussion of those procedures.

After selection of the fabric to be tested, the fabric samples were cut to accommodate the sample holder described in Chapter II. The dimensions of these samples were approximately 6-3/4 inches by 6-3/4 inches. The frame of the sample holder allows a six inch by six inch area of the sample to be exposed to the radiant heat source. Ten holes were also punched into the fabric sample to accommodate the ten screws of the sample holder.

With the fabric sample in place, the sample holder was secured between the two side plates of the sample holder assembly with four fastening screws. The entire assembly, shown in Figure 11, was placed in the environmental chamber for a minimum of 24 hours. The relative humidity of the chamber was adjusted to 30 percent, and the temperature was adjusted to 74°F.

Wood Sample Preparation

Two thermally thick materials were tested: western fir and construction plywood. The results of these tests are discussed in Chapter IV.

The thermally thick samples tested were cut to measure 6-1/2 inches by 6-1/2 inches. The sample holder used for

fabrics was also used for the thermally thick samples, and as mentioned above it provides a six inch by six inch area of the sample for exposure to the radiant heat source. These samples were secured in the sample holder, and the assembly was then placed in the environmental chamber for a minimum of 24 hours prior to test. The chamber's relative humidity and temperature were adjusted to 30 percent and 74°F, respectively.

Ignition Time and Ignition Frequency

Measurement Procedures

LITA can be operated in two modes: the ignition time test mode and the ignition frequency test mode. As discussed in Chapter II, in the ignition time test mode the sample is exposed to the radiant heat source at fixed exposure conditions for an indefinite exposure time to obtain the material ignition time. In the ignition frequency test mode the sample is exposed to the radiant heat source at fixed exposure conditions for a preselected interval. Several exposures are conducted at each time interval to obtain the fraction of ignitions. The procedures used for measuring ignition times of thermally thin and thick samples are the same. Likewise, the procedures used for measuring ignition frequencies of thermally thin and thick samples are the same. The remainder of this chapter is a description of these two sets of procedures.

Ignition Time Measurement Procedures

Before performing a group of ignition time measurements the following tasks were performed:

(i) The three electric contactors in the laboratory service corridor were turned on.

(ii) All instrumentation was turned on at least fifteen minutes prior to test to allow for component warm-up and check-out.

(iii) The air supply line was purged. This was accomplished by fully opening the air supply purge valve for a minimum of five minutes.

(iv) Air was supplied to the heaters by fully opening the heater air supply valve. The air pressure was checked for a minimum pressure of ten psig.

(v) The accumulator air supply valve was fully opened, and the pressure regulator was adjusted to 30 psig.

(vi) Cooling water was supplied to the heaters by fully opening the water supply valve. The mercury manometer was checked for a reading of at least 4.2 inches of mercury. (This reading corresponds to a total cooling water flow rate of 4.8 gallons per minute.)

(vii) The two infrascopes cameras were positioned as follows. The Mark I infrascopes was aimed between heaters number four and five. The Temptron infrascopes was aimed between heaters number three and four. Both infrascopes were focused on the centerline of a paper grid. This grid

was mounted on a plywood sample secured in the sample holder assembly. The sample holder assembly was located in front of the heater stack in the usual manner. The Mark I infrascopes were focused on a point 5.0 cm above the bottom edge of the exposed sample area. The Temptron infrascopes were focused on a point 13.5 cm above the bottom edge of the exposed sample area. The grid and sample holder assembly were then removed.

(viii) The radiant heater stack was preheated at 50 VAC load voltage for two minutes. This was accomplished by switching on the heater power breaker switches and rotating the variac control arm until a 50 VAC reading was observed on the voltmeter. After this preheat period the control arm of the variac was returned to the zero voltage position, and the heater power switches were turned off. The purpose of this procedure is to reduce the thermal shock of the heater bulb filaments during actual tests. This procedure was repeated if the heaters sat idle for more than fifteen minutes.

The procedures presented in the remainder of this section were performed for each ignition time measurement. Graph paper was placed in the X-Y plotter. Both channels were zeroed as prescribed by the plotter operating manual. The gains of the two Y channels were adjusted as indicated by the infrascopes outputs of previous tests. The gain of the sweep drive unit was adjusted to an expected ignition time.

A visual check was made to establish that the following switches and controls were in their pre-test positions:

- (i) the variac arm in the zero voltage position,
- (ii) the arming switch turned off,
- (iii) both air cylinder solenoid valve toggle switches turned off,
- (iv) the ejector assembly toggle switches turned off,
- (v) the six heater power breaker switches turned off,
- (vi) the mechanical block pinned in the retracted position, and
- (vii) the preheat toggle switch in the automatic position.

Both shutters were then locked into their respective shutter holder assemblies. The sample holder assembly with the attached sample was positioned in front of the heater stack.

The power button on the control panel was turned on. The idle heater voltage was adjusted to correspond with the selected steady state incident heat flux. (Steady state incident heat flux is plotted as a function of idle heater voltage as discussed in Chapter IV.) This was accomplished by rotating the variac arm until the selected idle heater voltage was observed. The power button was then turned off.

The preheat timer was adjusted by rotating the dial to the preheat time required for the selected steady state incident heat flux. This preheat time is determined from Figure E.1 in the Appendix.

At this point the apparatus and the instrumentation were ready to conduct a test. The following procedures were then followed:

- (i) the six heater power breaker switches were turned on,
- (ii) the arming switch was turned on,
- (iii) the fan power toggle switch was turned on,
- (iv) the sweep drive unit was turned on, and
- (v) the main power button was turned on.

The last procedure starts the preheat timer. After the preselected preheat time elapsed, the bottom shutter solenoid valve was actuated by the preheat timer. The bottom air cylinder then actuated accelerating the bottom shutter downward. The sample was then exposed to the radiant heat flux.

The sample was exposed to the radiant heat flux until ignition was recorded by the X-Y plotter. After ignition the main power button was turned off and all switches returned to their respective pre-test positions.

After ignition the sample can be disposed into the receptacle by turning on the disposal toggle switch located on the control panel. This procedure was not used with the fabric and wood samples tested since none of the samples

continued to burn more than ten seconds after the heater power was turned off.

Ignition Frequency Measurement Procedures

As discussed in Chapter IV, ignition frequency measurements were only conducted on the 65 percent polyester/35 percent cotton fabric. The ignition frequency measurement procedures used for this fabric are also applicable to other thermally thin and thermally thick materials.

The ignition frequency measurement procedures are identical to the ignition time measurement procedures with the following exceptions: Before conducting a group of ignition frequency measurements, the test mode toggle switch was set in the exposure time position. Also, since the sample was only observed visually for ignition, the X-Y plotter, the two infrascopes, and the sweep drive unit were not used during any portion of the test.

Before each ignition frequency measurement, the Fisher micro-timer on the control panel was reset in the zero position. With all switches and controls positioned for test as discussed in the previous section, the following procedures were conducted for each ignition frequency measurement:

(i) The main power button was turned on. This started the preheat timer. After the selected preheat time had elapsed, the bottom air cylinder solenoid valve actuated. The bottom shutter was then accelerated downward

by the bottom air cylinder. When the bottom shutter deflected the arm of the lower, bottom shutter micro-switch, the micro-timer was started. As discussed previously, this operation corresponded to the instant the top edge of the shutter was even with the top of heater number six. (This location corresponds to the lower boundary of the uniform heating area described in Chapter IV.)

(ii) After the preselected exposure time had elapsed as monitored by the micro-timer, the top shutter solenoid valve toggle switch was turned on manually. The top air cylinder solenoid valve then actuated. The top air cylinder accelerated the top shutter downward terminating exposure of the sample to the radiant heat source. When the top shutter contacted the impact bar assembly, the arm of the lower, top shutter micro-switch was deflected. (The top of the impact bar assembly is 13 cm below the lower boundary of the uniform heating area.) The signal from this micro-switch then stopped the micro-timer.

(iii) After turning off the main power button, the sample was visually observed for ignition.

(iv) All switches and controls were returned to their respective pre-test positions.

CHAPTER IV

RESULTS AND DISCUSSION

This chapter summarizes the results of:

- (i) the heat flux measurements of the radiant heater stack,
- (ii) the top and bottom shutter velocity tests,
- (iii) the total heater current measurements,
- (iv) the fabric ignition time measurements,
- (v) the fabric ignition frequency tests, and
- (vi) the wood ignition time measurements.

In addition, visual observations made during the fabric and wood ignition time tests are discussed.

The Heat Flux Measurements of the Radiant Heater Stack

The steady state incident heat flux of the radiant heater stack was measured at 35 locations with 204 VAC idle heater voltage. As discussed in Chapter III, these locations were spaced evenly over the entire heating area. The sensor was positioned to coincide within 1/16 inch of the sample plane which is 5.1 cm (two inches) in front of the heater windows. Comparison of the heat flux measurements shows that a heating area 30 cm wide and 38 cm long is uniform within one percent. The upper boundary of this

uniform heating area coincides with the top of heater number two. The lower boundary of this uniform heating area coincides with the top of heater number six. As a check on these conclusions, steady state incident heat flux was measured at 18 locations with 105 VAC idle heater voltage. As discussed in Chapter III, these locations were spaced evenly in front of the top half of the heating area in the sample plane. Similar to the first set of measurements, the upper boundary of the uniform heating area coincided with the top of heater number two. In addition, the width of the uniform heating area was also 30 cm. These two sets of measurements indicate that the size of the uniform heating area does not vary for a change in the radiant heating intensity.

The steady state, incident, radiative heat flux and the preheat time required by the heaters to attain steady state operation were measured for idle heater voltages between 50 VAC and 200 VAC in increments of 10 VAC. These results are plotted in Figure E.1 of the Appendix. This figure indicates a maximum incident heat flux of 16.8 watts per cm^2 was measured at 204 VAC idle heater voltage. This compares to the manufacturer's published value of 20.5 watts per cm^2 at a rated voltage of 240 VAC. Thus the maximum incident heat flux is restricted by the 208 VAC laboratory voltage presently available. A significant increase in heat flux could be obtained by increasing the laboratory voltage

to 240 VAC as recommended in Chapter V, if higher heat flux intensities are required.

Shutter Velocity Tests

The bottom and top shutter velocities were measured using the procedures detailed in Chapter III. For an accumulator pressure of 30 psig, the average velocity of the bottom shutter is 320 cm per second. This average velocity corresponds to the portion of travel (of the top edge of the shutter) bounded by the top of heater number two and the top of heater number six. For an accumulator pressure of 30 psig, the average velocity of the top shutter is 323 cm per second. This average velocity corresponds to the portion of travel (of the bottom edge of the shutter) bounded by the top of heater number two and the top of the top impact bar assembly.

For a six inch high sample, a velocity of 320 cm per second corresponds to an exposure transient of 48 milliseconds. For the same size sample, a velocity of 323 cm per second corresponds to an exposure transient of 47 milliseconds. Thus for samples six inches high with ignition times greater than 4.8 seconds, an accumulator pressure of 30 psig results in exposure transients less than one percent of ignition time.

For a sample 38 cm high which would cover the constant heat flux region, a velocity of 320 cm per second corresponds

to an exposure transient of 115 milliseconds. For the same size sample, a velocity of 323 cm per second correspond to an exposure transient of 112 milliseconds. Thus for samples 38 cm high with ignition times greater than 11.5 seconds, an accumulator pressure of 30 psig results in exposure transients less than one percent of ignition time.

Total Heater Current Measurements

The total heater current was measured at various idle heater voltages as a check on the heater performance. The maximum current measured was 209 amps with an idle heater voltage of 204 VAC. The complete results of these measurements are listed in Table E.1 of the Appendix. In comparison, the total current of the six heaters operating at a rated voltage of 240 VAC is 240 amps.

Summary of Fabric Ignition Time Measurements

Twenty six ignition time measurements were conducted on five fabrics. Four of these fabrics were selected from the group known as the "ten primary GIRCFF fabrics." These ten fabrics were chosen by the Government-Industry Research Committee on Fabric Flammability on the basis of frequency of use. These fabrics are listed in Table II-1 of Reference [5]. The fifth fabric tested was obtained from the School of Textile Engineering. This fabric, a 100 percent cotton weave, was not treated chemically during manufacture.

The five fabrics tested are:

- (i) shirting (white), 50 percent polyester/
50 percent cotton, GIRCFF number 16,
- (ii) batiste (white), 65 percent polyester/
35 percent cotton, GIRCFF number 17,
- (iii) flannel (white), 100 percent cotton,
GIRCFF number 18,
- (iv) flannel (navy blend), 100 percent wool,
GIRCFF number 20, and
- (v) twill weave, 100 percent cotton (obtained from
the School of Textile Engineering).

Physical properties of the four GIRCFF fabrics are listed in Table C.1 of the Appendix. Other physical properties have been presented in Reference [7].

The ignition times of these fabrics were obtained from the two infrascopes outputs recorded by the X-Y plotter. Two infrascopes output history plots of a typical fabric ignition time measurement are shown in Figure 13. The top curve represents the output of the Temptron infrascopes which was focused on the sample at a point 13.5 cm above the bottom edge of exposed sample area. The bottom curve represents the output of the Mark I infrascopes which was focused on the sample at a point 5.0 cm above the bottom edge of the exposed sample area. Both of these points coincided with the vertical centerline of the sample. The quantitative values of the infrascopes outputs are of no

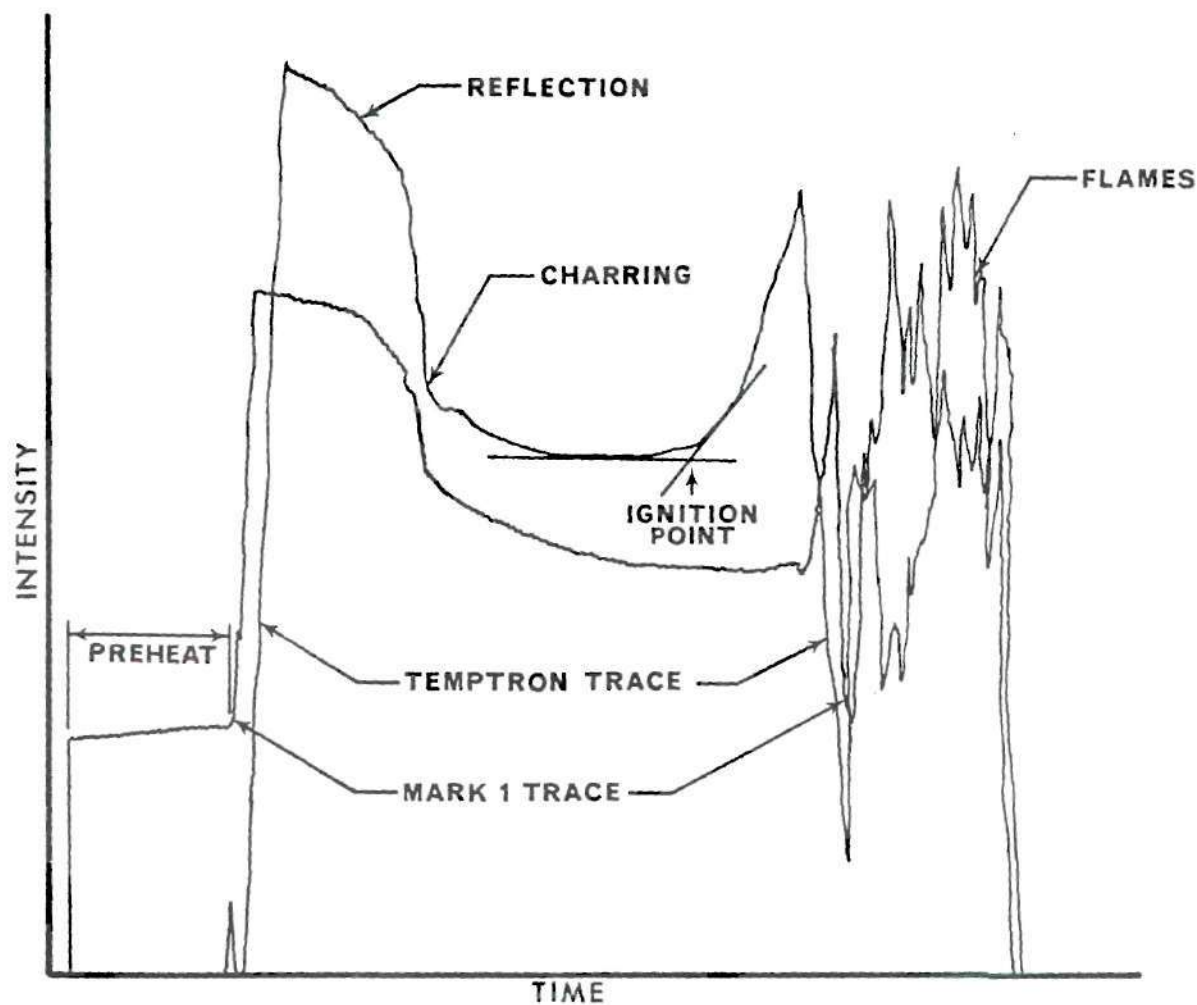


Figure 13. Infrascop Output History Plots; GIRCFF Fabric Number 17 Exposed to an Incident Heat Flux of 15.7 W/cm^2 ; Temptron Focused at 13.5 cm and Mark I at 5.0 cm above the Bottom Edge of Sample

significance for the present measurements. However the change in these outputs provides the following information:

(i) The initial step in the top curve represents the preheat period of the radiant heater stack. This increase in output of the bottom infrascopes is due to reflection of the heat flux off the bottom shutter. For the top infrascopes the lower segment of the scale is suppressed.

(ii) The sudden and large rise in both curves represents initial exposure of the sample. This is due to reflection off the sample as recorded by the infrascopes.

(iii) The gradual decline of both curves records the decrease in output of the two infrascopes due to the reduced reflectance of the sample. This reduction in reflectance is the result of charring of the sample.

(iv) The sudden rise in both curves indicates ignition which is defined as the appearance of a flame. The ignition point is the intercept of the tangent to the portion of the curve that represents char formation and the tangent to the portion of the curve that represents thermal excursion.

(v) The remainder of each curve, characterized by sudden fluctuations, records flames and smoke generation. The sudden decline of both curves records the termination of heater power.

Knowing the time base, the ignition time is calculated from the distance between the sudden jump in the curve, representing initial exposure and the ignition point. The

distance between the starting points of the two curves is due to the off-set design of the two-pen recorder. The initial exposure point of the curve recorded by the Temptron infrascopes is determined using the latter distance and the step of the curve recorded by the Mark I infrascopes. As evidenced in Figure 13, the top infrascopes usually recorded a shorter ignition time than did the bottom infrascopes. This indicates that the flame propagated downward.

The infrascopes output history plots of another fabric ignition time test are shown in Figure C.1 of the Appendix. This fabric, GIRCFF number 20, was exposed to an incident heat flux of 15.8 watts per cm^2 . The characteristic portions of both curves are similar to those of Figure 13.

The results of the ignition time measurements are summarized in Table C.2 of the Appendix. For each fabric tested with LITA, the only parameter varied was the heating intensity. Most of the heating intensities were selected to coincide with the heating intensities used previously with the Radiative Ignition Time Apparatus (RITA) [6,7,8]. RITA, which is described in Reference [5], exposes fabric samples of 25 mm diameter to a uniform radiant heat source. The heat source is an RI Controls, model 5208-5, radiant heater. RITA also has a dual shutter system which provides exposure transients less than one percent of ignition time at both the start and end of exposure. The results of the tests conducted with RITA have been reported in References

[6,7,8], and they are also summarized in Table C.2.

Comparison of fabric ignition times measured using LITA and RITA shows the effect of fabric size on ignition time. (As stated previously, the exposed area of all the samples tested using LITA measured 152 mm by 152 mm (six inches by six inches).)

The results of the above tests are also normalized according to modeling rules described in Reference [5]. The parameters that evolved from this analysis are:

- (i) the non-dimensional ignition time or Fourier number

$$(N_{Fo})_i = \frac{(k/\delta)\tau_i}{c(\rho\delta)} \quad (4)$$

and

- (ii) the non-dimensional radiative heat flux or Biot number

$$(N_{Bi})_r = \frac{(1-\tilde{\rho})W_o}{(k/\delta)(T_i-T_o)} \quad (5)$$

where (k/δ) , τ_i , c , $(\rho\delta)$, $\tilde{\rho}$, W_o , T_i , and T_o are respectively the thermal conductance, the ignition time, the specific heat, the mass per unit area, the reflectance, the radiative incident heat flux, the self-ignition temperature, and the environment temperature. For all the tests conducted, the

environment temperature was 24°C.

Figure 14 is a normalized plot of the LITA and RITA ignition time tests for the four GIRCFF fabrics. Figures 15-18 are separate plots of the LITA and RITA tests for each of the GIRCFF fabrics.

A comparison of the LITA and RITA fabric tests indicates that the ignition times of GIRCFF fabrics, number 16, 17 and 20, decrease as the sample size increases. Particularly significant was the decrease in ignition time of GIRCFF fabric number 20. For this fabric, the 152 mm by 152 mm size samples ignited in less than half the ignition time of the 25 mm diameter size samples for the same heating intensities. This difference is evidenced by the shift to the lower left of the LITA normalized data compared to the RITA normalized data as shown in Figure 18.

GIRCFF fabric number 18 did not follow this trend of smaller ignition times for a larger sample at all heating intensities. At the higher heating intensities (9.0 and 14.3 watts per cm²) the samples tested with RITA ignited sooner than did the samples tested with LITA as evidenced by Figure 17. However, at the lowest heating intensity (5.7 watts per cm²) the larger sample tested with LITA ignited in less time than did the sample tested with RITA.

During the ignition time tests of the five fabrics, several general observations were noted. These observations were made by visually inspecting the fronts of the fabrics

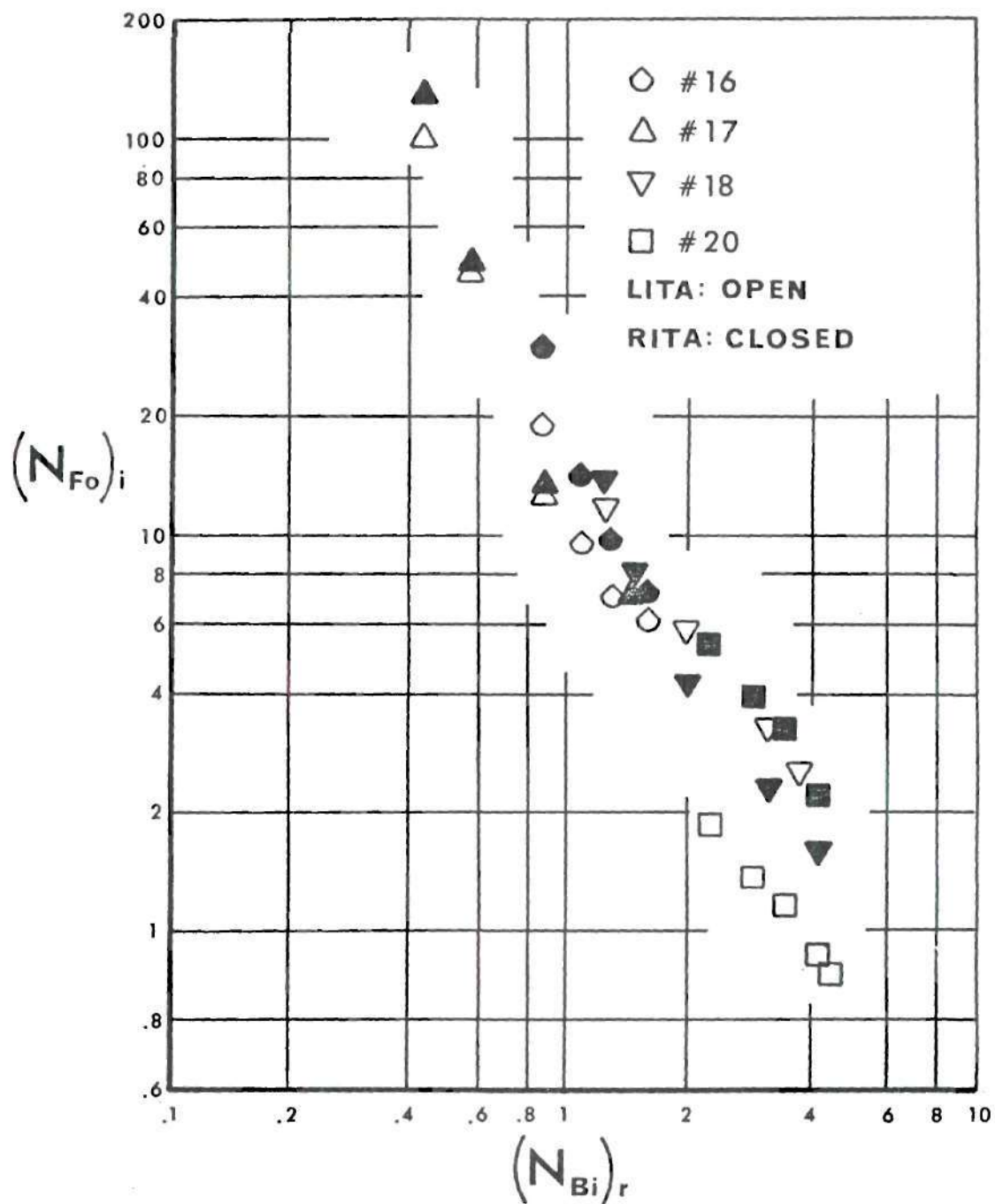


Figure 14. Normalized Plots of the LITA and RITA Fabric Ignition Time Measurements

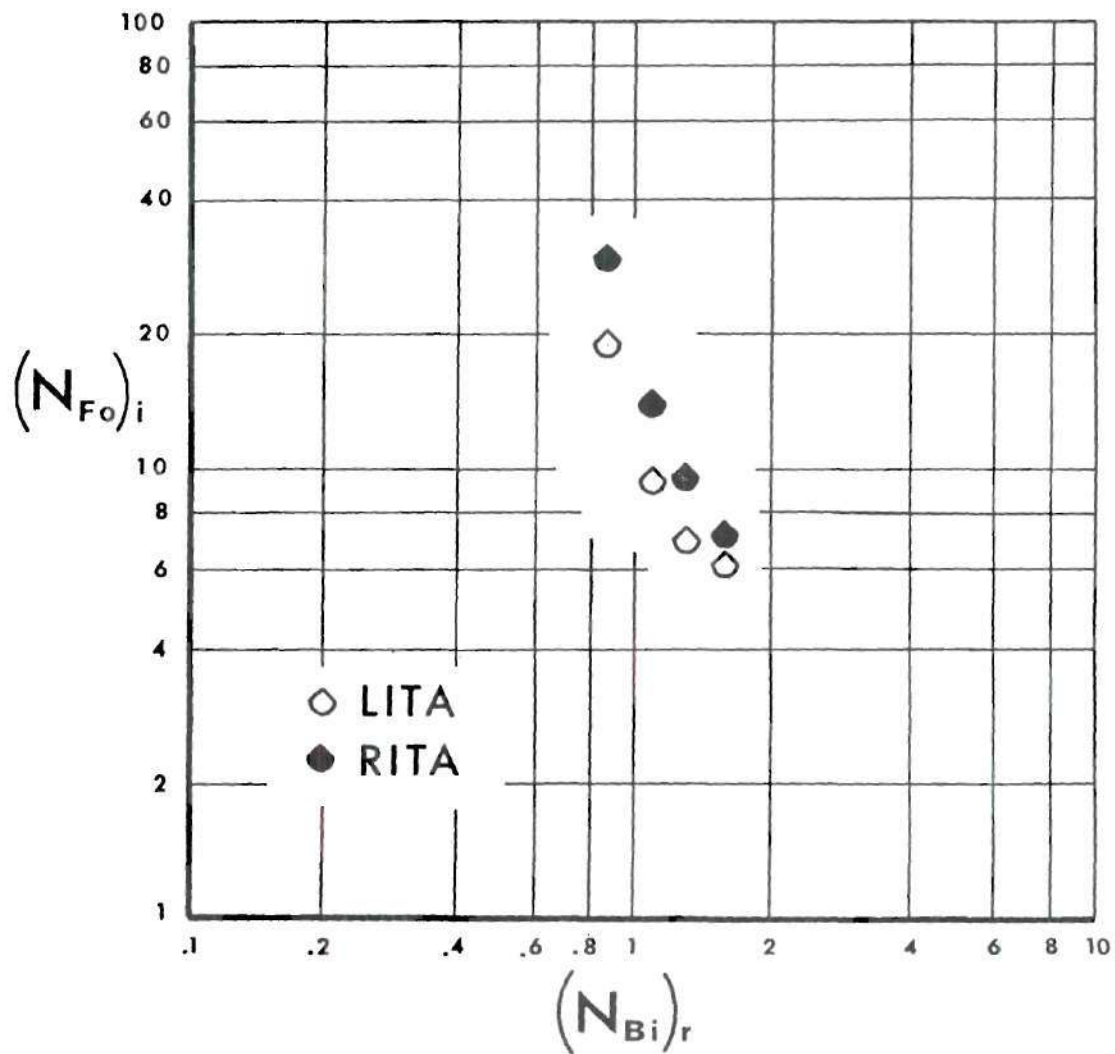


Figure 15. Normalized Plots of the LITA and RITA Ignition Time Measurements of GIRCFF Fabric Number 16

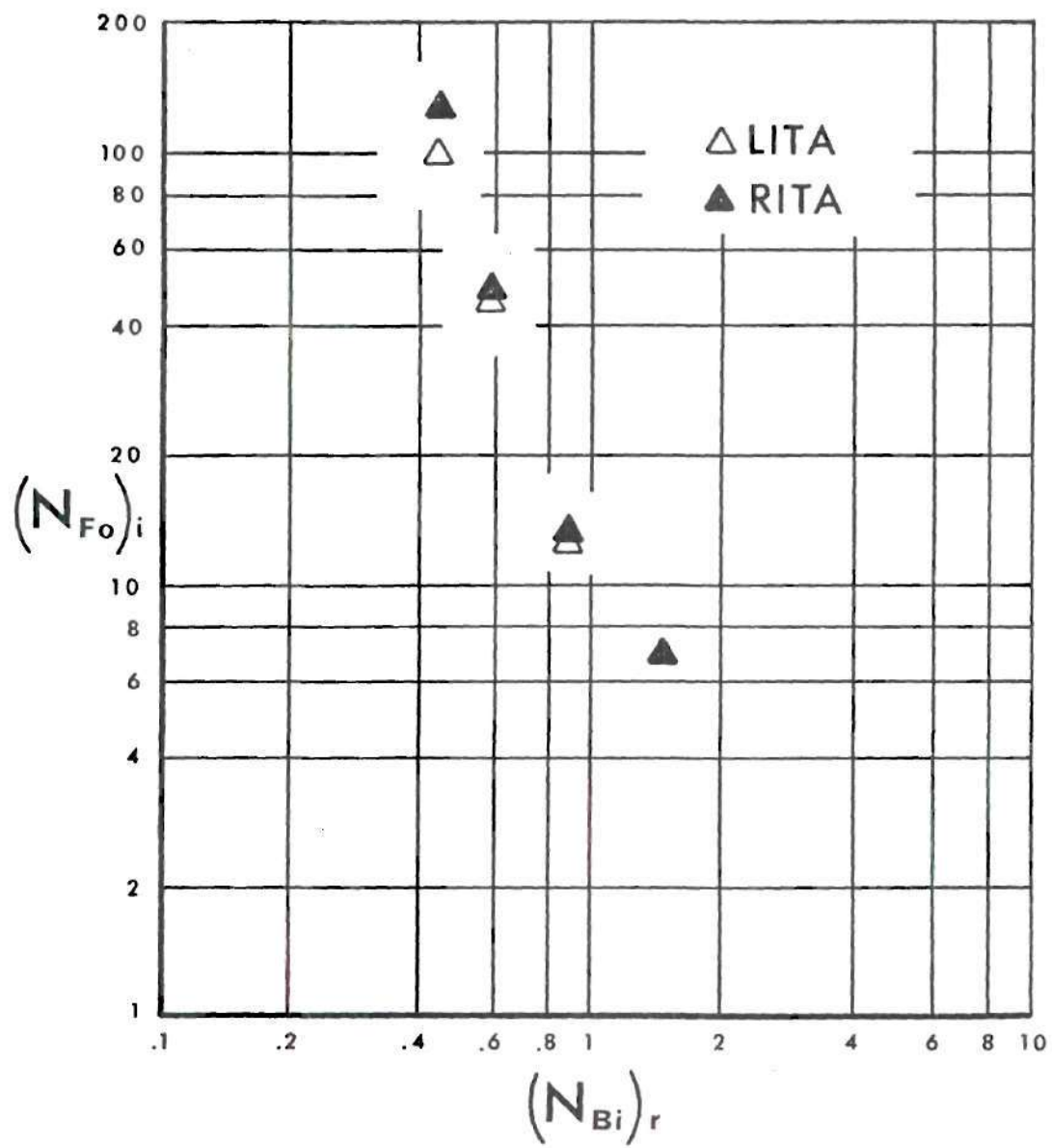


Figure 16. Normalized Plots of the LITA and RITA Ignition Time Measurements of GIRCFF Fabric Number 17

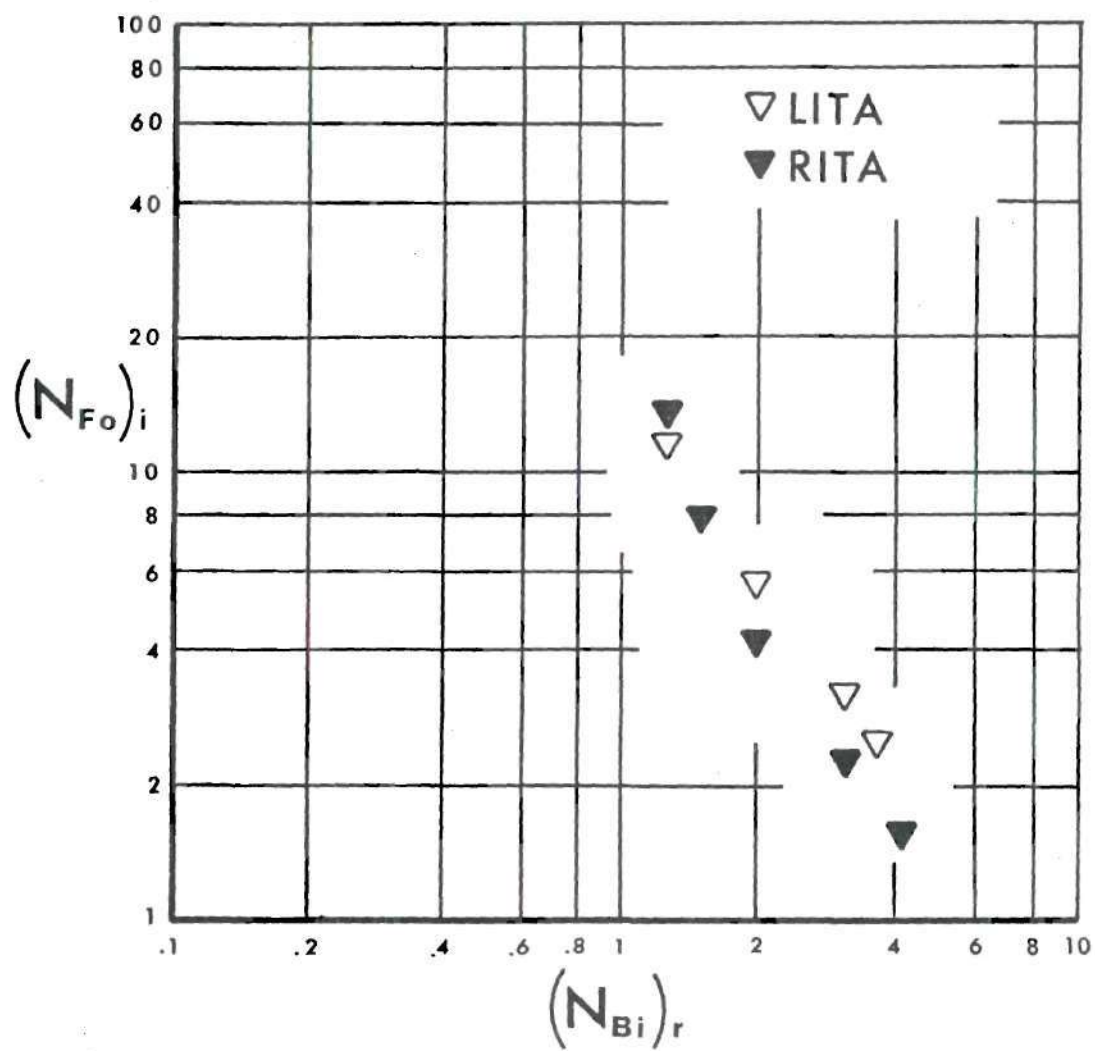


Figure 17. Normalized Plots of the LITA and RITA Ignition Time Measurements of GIRCFF Fabric Number 18

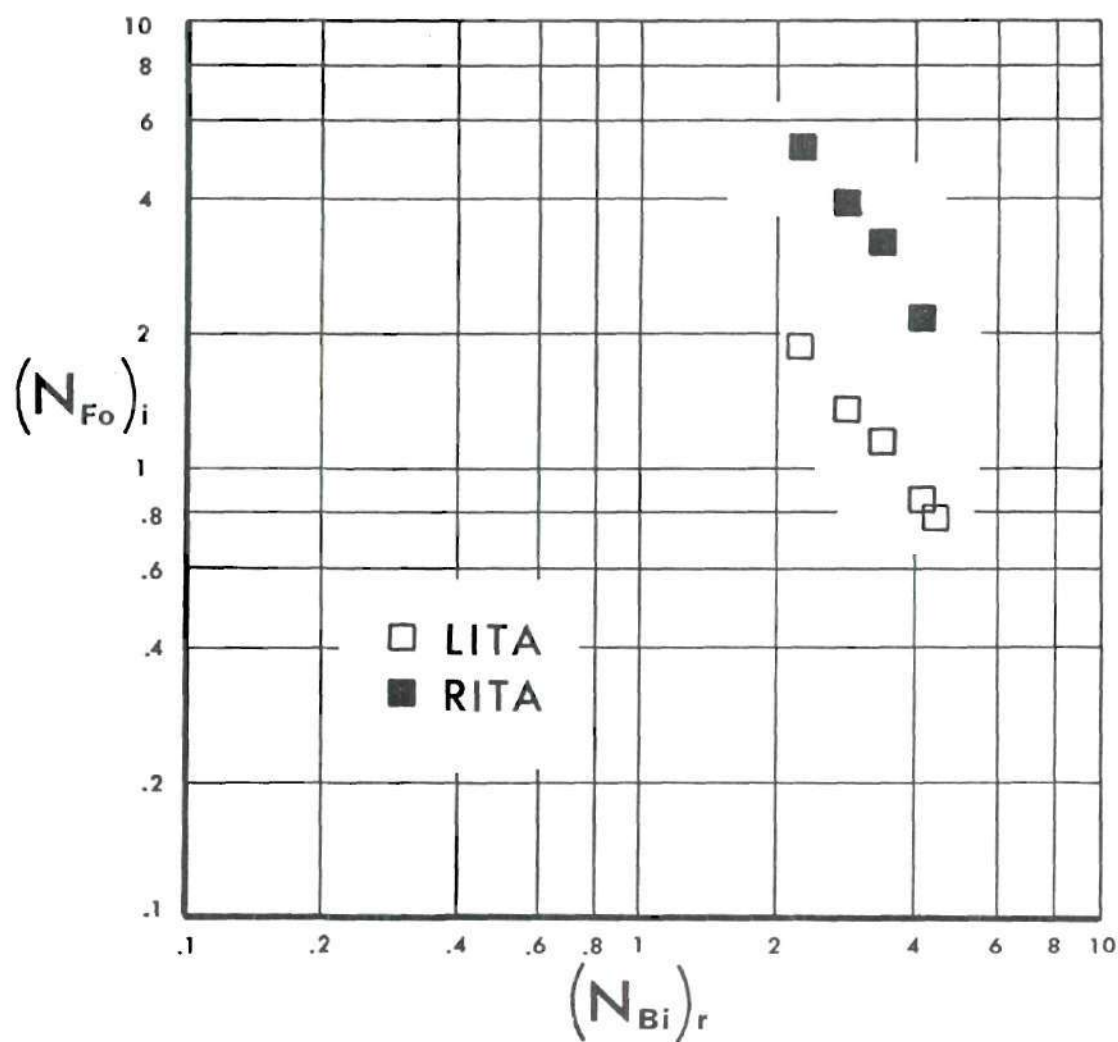


Figure 18. Normalized Plots of the LITA and RITA Ignition Time Measurements of GIRCFF Fabric Number 20

through the 1/4 inch heater gaps and from the side of the structure. The backs of the samples were also observed by looking at a mirror mounted behind the structure.

All of the fabrics tested followed a similar pre-ignition process. After exposure to the heat source, the reflectance of the fabric sample continually decreased. This decrease in reflectance is attributed to charring of the fabric sample. After an initial period of char formation, smoke generation became prominent and immediately prior to ignition increased significantly.

All of the fabrics exhibited gaseous phase ignition. Ignition was observed to initiate a few centimeters below the front top of the fabric sample and propagate downward. The only exception to this phenomena was that of the wool fabric, GIRCFF number 20. Immediately prior to ignition, the wool fabric sample disintegrated at several locations spaced evenly over the entire sample area. Furthermore a localized ignition point for the wool samples could not be ascertained.

The two polyester/cotton blends also exhibited individual ignition characteristics. Prior to ignition, sagging and melting of these fabric samples was observed. The location of initial melting was also a few centimeters below the top edge of the sample.

In summary, a review of the fabric ignition time tests indicates that larger samples ignite sooner than do smaller

ones for the same heating intensity and that ignition is a gaseous phase phenomena originating at the top of the sample. These conclusions can probably be explained by the greater heat absorption and pyrolysate generation per unit width of the larger sample. Hence, the temperature and pyrolysate concentration at the top of the larger sample would, because of convection, increase faster. This would account for the shorter ignition times of the larger samples and would account for the location of ignition. The behavior of fabric number 18 cannot be explained at this point. Additional tests are needed to investigate its behavior.

Summary of Fabric Ignition Frequency Tests

In addition to the ignition time tests, two ignition frequency tests were conducted on GIRCFF fabric number 17 to verify the operation of LITA in this mode. At a heating intensity of 15.7 watts per cm², the sample ignited after an exposure of 8.0 seconds. At the same heating intensity, the sample charred but did not ignite after an exposure period of 7.2 seconds. Though more data is necessary for significant ignition frequency statistics, these results verified the feasibility of conducting ignition frequency tests.

Summary of Wood Ignition Time Measurements

Ignition time measurements were conducted on 26 samples of two thermally thick materials: western fir and

construction plywood. Properties of these materials are listed in Table D.1 of the Appendix.

An area of six inches by six inches of 3/4 inch samples of western fir and plywood were exposed to heat flux levels of 6.0, 8.0, 12.0, 14.0, and 16.8 watts per cm^2 . Similarly, 1/4 inch and 1/2 inch samples of plywood were exposed to these same heating intensities.

The ignition time measurements on the wood samples were obtained using procedures identical to those for the fabric ignition time tests. Figure 19 shows the infrascopes output history plots of a typical wood ignition time test. This test was conducted on 1/2 inch plywood exposed to a heat flux of six watts per cm^2 . The curves plotted in Figure 19 are similar to those of Figure 13. The major difference between these two sets of curves is the more pronounced rise of the curves representing ignition of the wood sample. This difference is due to the larger time base of the wood ignition time test. Figure D.1 of the Appendix shows the infrascopes output history plots of a test conducted on 1/2 inch plywood exposed to a heat flux level of 8.0 watts per cm^2 .

The results of the wood ignition time measurements are summarized in Table D.2 of the Appendix. As listed in this table, two of the tests resulted in no ignition. Of two tests conducted on 1/2 inch plywood samples exposed to a heat flux of 6.0 watts per cm^2 , one sample did not ignite.

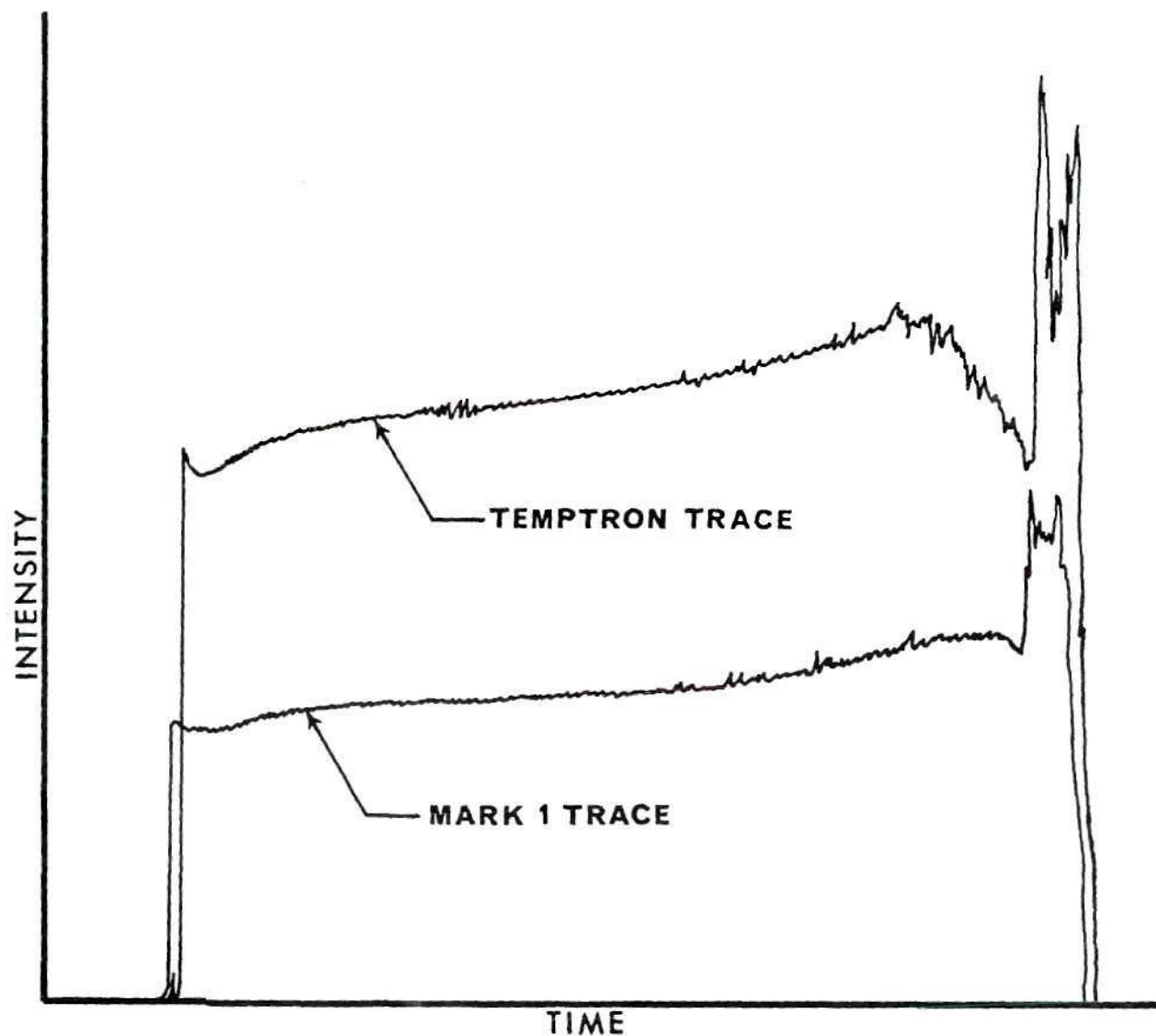


Figure 19. Infrascopes Output History Plots; 1/2 Inch Plywood Exposed to an Incident Heat Flux of 6.0 W/cm^2 ; Temptron Focused at 13.5 cm and Mark I at 5.0 cm above the Bottom Edge of the Sample

The results of this test are shown in Figure 20. As indicated in this figure, the rise in the curves is attributed to glowing of the char. One of the two tests conducted on 3/4 inch western fir exposed to a heat flux of 6.0 watts per cm^2 also resulted in no ignition.

The ignition time measurements of the wood samples are normalized using equations (4) and (5). The normalized plots are shown in Figure 21. The environment temperature, T_0 , was 24°C.

Comparison of the plywood sample data results in the following observation. For a given heating intensity, an increase in thickness corresponds to a decrease in ignition time. Initially this correlation was attributed to convective cooling off the back of the sample. However, a review of an inert heating model shows that convection from the unexposed side of the material is not significant at these heating rates [5]. The model referred to accounts for inert heating of the front face of the sample and includes convective heat losses from the back of the sample. An explanation for this phenomena might be found from a study of:

- (i) the pyrolysate generation process, and
- (ii) the heating and air-fuel mixing process in the thermal boundary layer.

Such an investigation is, however, beyond the scope of this work.

The effect of thickness is also evident in the plots

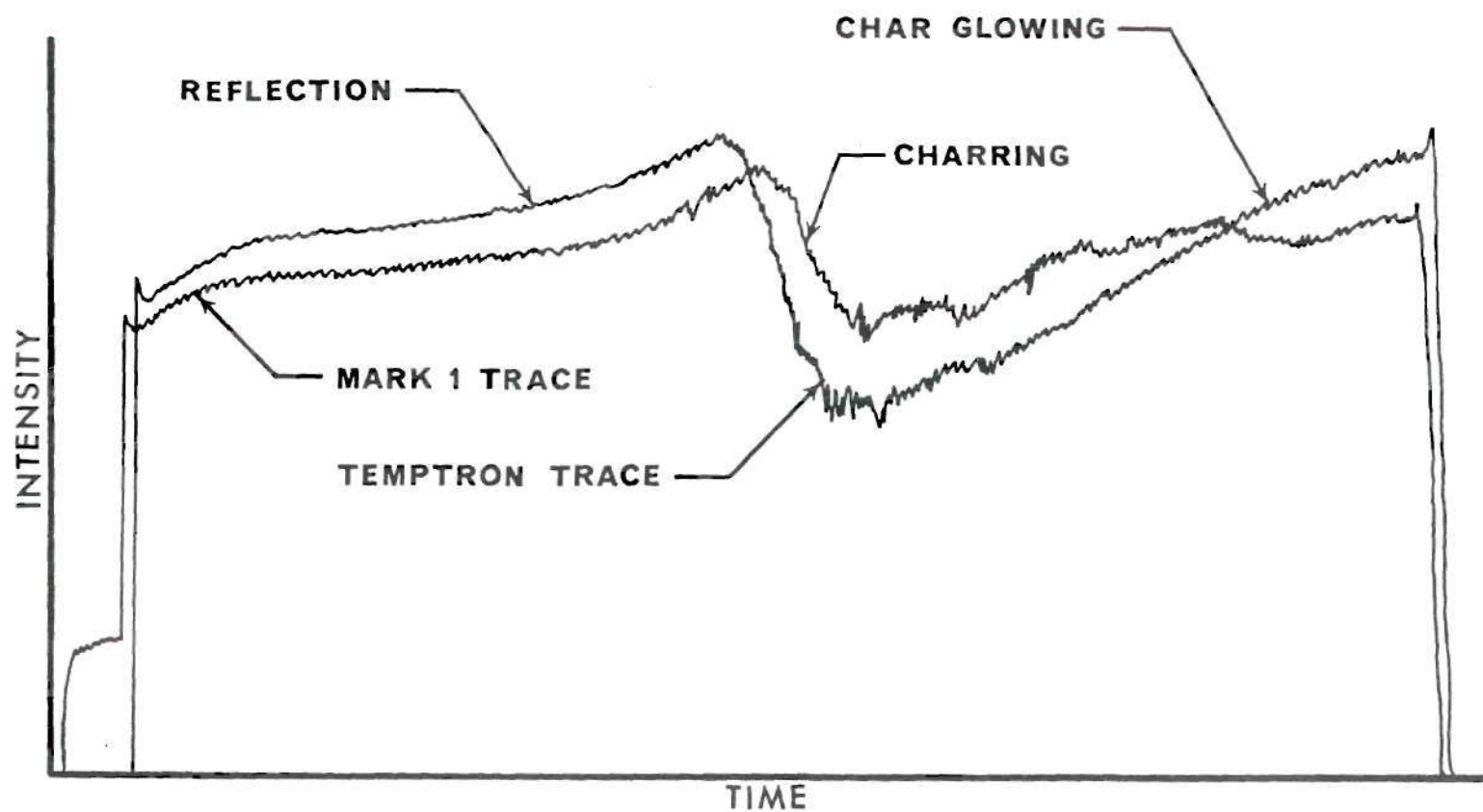


Figure 20. Infrascopes Output History Plots; 1/2 Inch Plywood Exposed to an Incident Heat Flux of 6.0 W/cm^2 ; Temptron Focused at 13.5 cm and Mark I at 5.0 cm above the Bottom Edge of the Sample

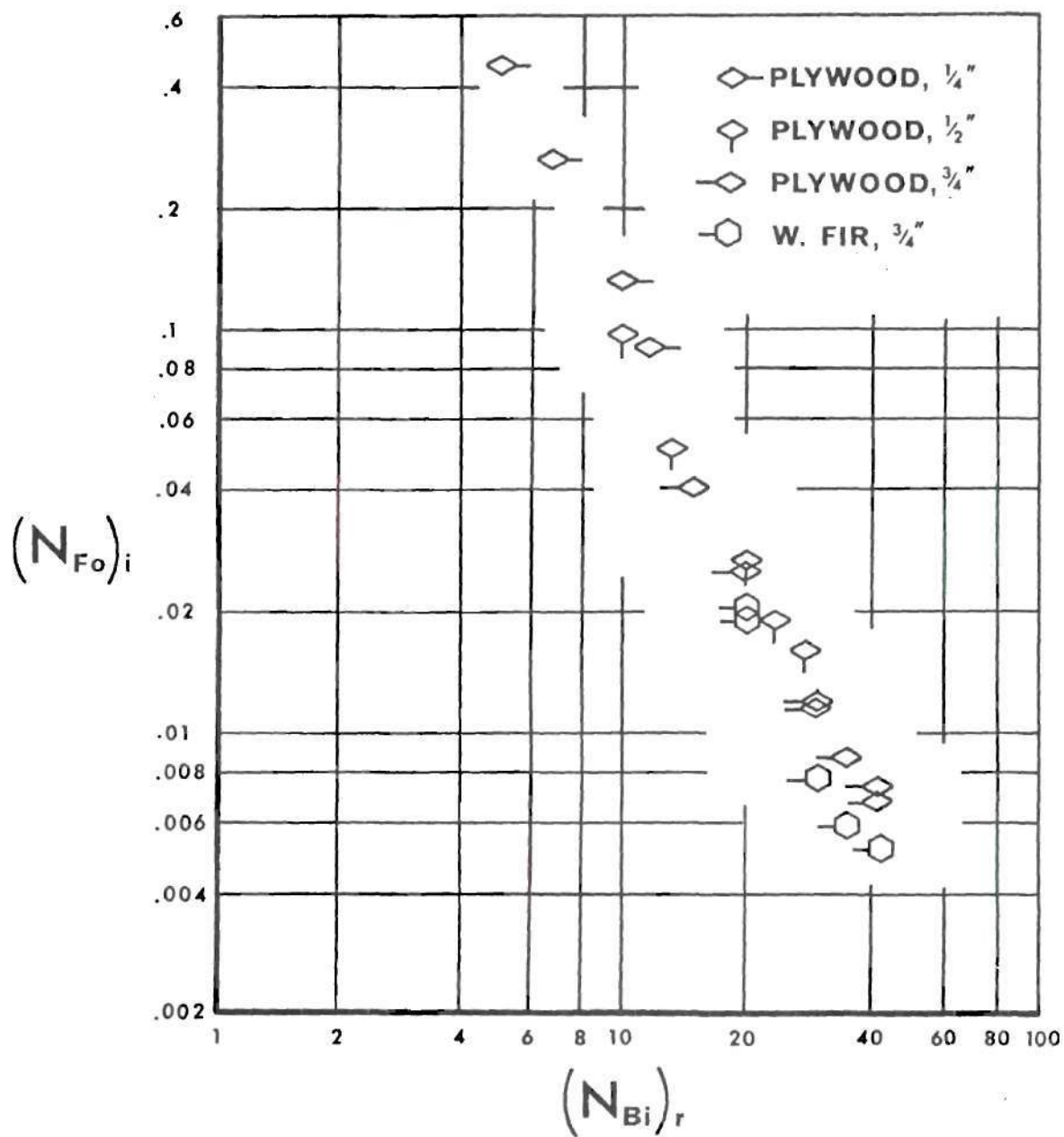


Figure 21. Normalized Plots of the LITA Wood Ignition Time Measurements

shown in Figure 21. Also significant is the similarity of the 3/4 inch plywood and western fir normalized data. These results suggest a reasonable estimate of ignition time can be calculated using equations (4) and (5) and the pertinent thermophysical properties.

Several visual observations were made during the wood ignition time tests. As in the case of the fabrics, the wood samples exhibited significant char formation and smoke generation prior to ignition. Not surprisingly, however, the char formation and smoke generation were much more pronounced than that of the fabric samples.

Also, similar to the fabric samples, the wood samples were characterized by gaseous phase ignition. But because of the high velocity of flame propagation, the locality of ignition could not be definitely ascertained.

After ignition, flame jets were observed at several locations over the wood sample area. These jets had a diameter of about 1/16 inch and projected approximately 1/8 inch beyond the sample surface.

After the heater power was turned off, a flame at the bottom of the sample was observed. This flame self-extinguished within ten seconds after termination of the test.

Quarter sections of the 1/2 inch plywood samples were cut and visually inspected. (These samples ignited after exposure to the following heating intensities: 6.0, 8.0, 12.0, 14.0, and 16.8 watts per cm².) For these samples,

depth of charring and wood discoloration increased for a decrease in heating intensity (and hence increase in ignition time). However, even at the lowest heating intensity, the affected depth did not exceed the thickness of the first wood lamination. It was therefore concluded that the glue between the laminations did not pyrolyze. Furthermore, it appears that heat conduction beyond the first lamination is not significant.

Quarter sections of 1/4, 1/2, and 3/4 inch plywood samples were also cut and visually inspected for depth of char and wood discoloration. (Each of these samples was exposed to a heating intensity of 8.0 watts per cm².) The affected depth of these samples did not vary significantly. In all cases the depth of char was approximately 1/16 inch. This also suggests that heat transfer beyond the first lamination is not significant.

CHAPTER V

CONCLUSIONS AND RECOMMENDATIONS

This chapter briefly summarizes the major accomplishments of this work. Also presented are conclusions made from the fabric and wood ignition time tests. In addition, recommendations for further work are discussed.

Summary of Accomplishments

The major objective of this research effort was the design and construction of the Large Ignition Test Apparatus. This task has been successfully completed. LITA has been characterized as follows:

- (i) It provides uniform, time-invariant, radiative heating of samples in sizes up to 30 cm by 38 cm by 5 cm at heat fluxes between 0.25 and 16.8 watts per cm².
- (ii) Sample exposure transients are below one percent of ignition time at both the start and the end of the preselected exposure interval.
- (iii) Time exposure is manually controlled.
- (iv) It provides remote infrared detection of flames.

The successful operation of LITA in the ignition time test mode was verified by:

- (i) 28 ignition time tests conducted on five fabrics, and

- (ii) 26 ignition time tests conducted on construction plywood and western fir samples.

In addition, LITA was successfully operated in the ignition frequency test mode.

Conclusions on Observations and Recommendations
for Further Work

The major objective of the test program was to verify the operation of LITA in the ignition time and ignition frequency test modes. This objective was accomplished. In addition, several significant observations were made. Two of these observations suggest correlations between sample size and ignition time. Additional tests, which are recommended in the following paragraphs, are needed to confirm these correlations.

The first significant observation made concerns the effect of sample area on fabric ignition times. The results of the ignition time measurements conducted on GIRCEFF fabrics number 16, 17, and 20 indicate that an increase in sample size decreases ignition time. This effect is probably due to the greater amount of heat absorption and pyrolysate generation per unit width of the larger sample. Additional data from other size samples and other fabric materials is needed to definitely confirm the effect of sample size on ignition time. Furthermore, the effect of sample width for a given sample height could be checked.

The results of such an investigation would be helpful in future ignition time studies.

The second significant observation made concerns the effect of sample thickness on ignition times. A comparison of plywood sample ignition times indicates that an increase in sample thickness decreases ignition time. An explanation for this phenomena might be found in an analytic study of the heating and air-fuel mixing process in the thermal boundary layer. In addition to such a study, the effect of sample thickness on ignition time should be checked experimentally for other materials such as different woods and plastics. The effect of different backings on the ignition times of wood paneling could also be checked. This data would aid in the fire hazard description of these assemblies.

In addition to the correlation of ignition times and sample thicknesses, the results of the wood ignition time measurements suggest that radiative ignition times can be predicted if the thermophysical properties of a material are known. This conclusion is supported by the very definite trend of data plotted in Figure 21. Additional data obtained from other materials such as different woods and plastics are needed to confirm this opinion.

Another observation made during the wood ignition time measurements is the significant amount of smoke generation. Smoke generation probably has a significant effect on ignition time and is, therefore, worthy of investigation. The

attenuation of the heat flux due to smoke could be measured by mounting a heat flux sensor in the wood sample. If desired, this data could be used with an analytical model to better predict ignition times.

A final recommendation is presented in regard to the design. The maximum heat flux of the LITA heater stack could be increased significantly by rewiring the laboratory power lines. The maximum heat flux of 16.8 watts per cm^2 is restricted by the available laboratory supply voltage. By increasing this voltage to 240 VAC, a heat flux of approximately 20 watts per cm^2 could be obtained.

APPENDICES

APPENDIX A

ASSEMBLY DRAWINGS

This Appendix contains assembly drawings of the bearing assembly, the shutter support assembly, and the ejector assembly.

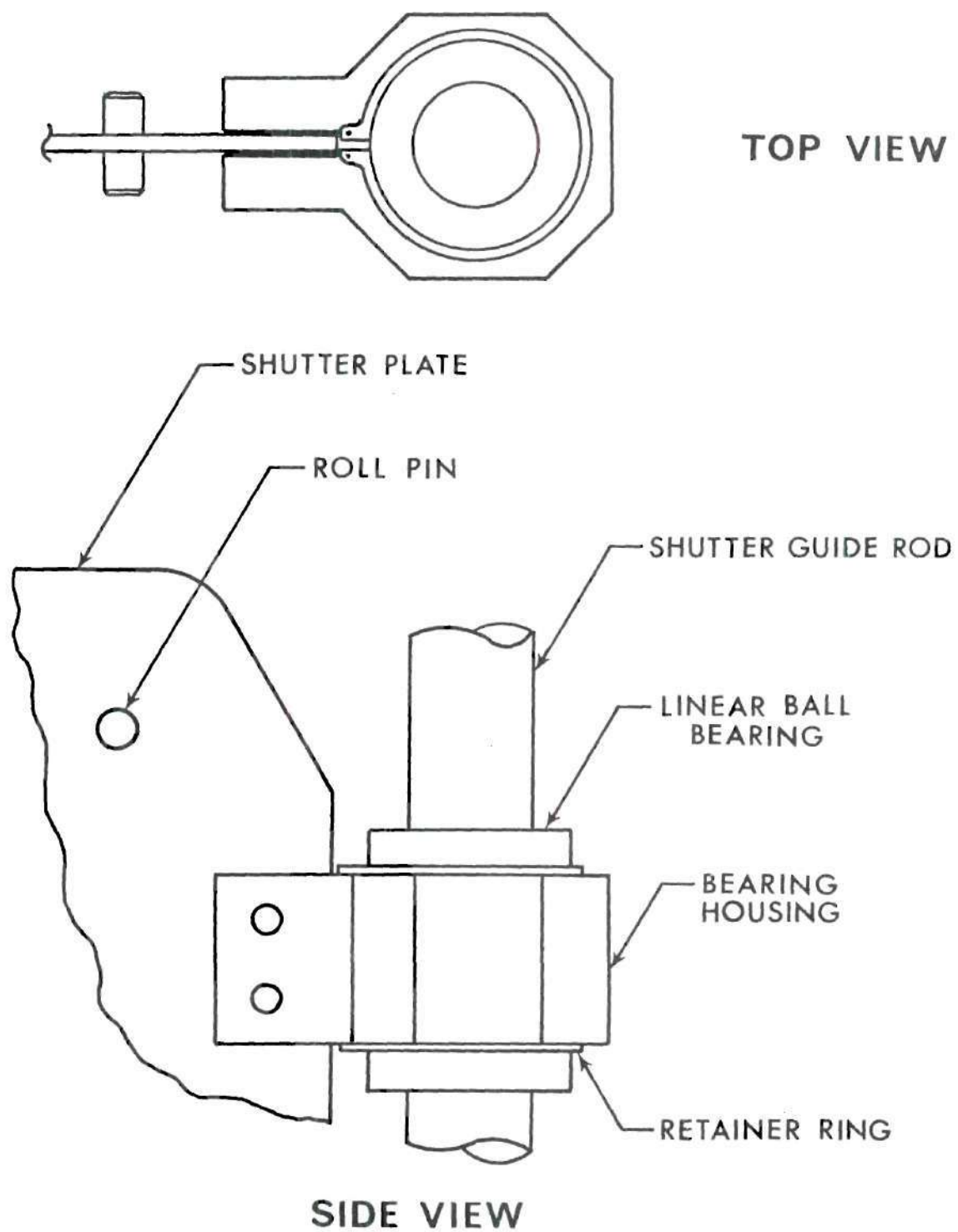


Figure A.1. Top and Side Views of the Bearing Assembly for Shutter Travel and Guide

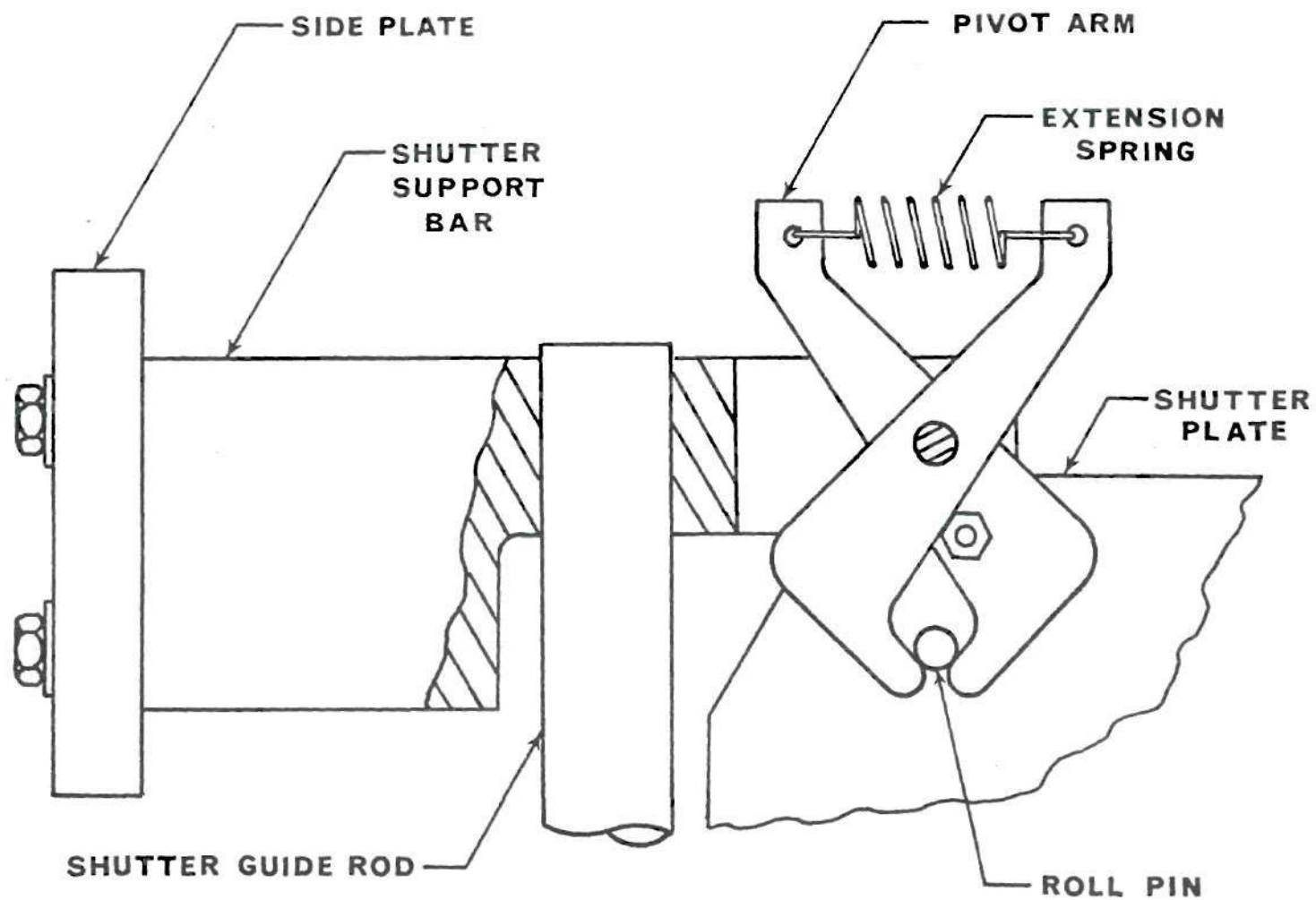


Figure A.2. Side View of the Shutter Support Assembly with Attached Shutter

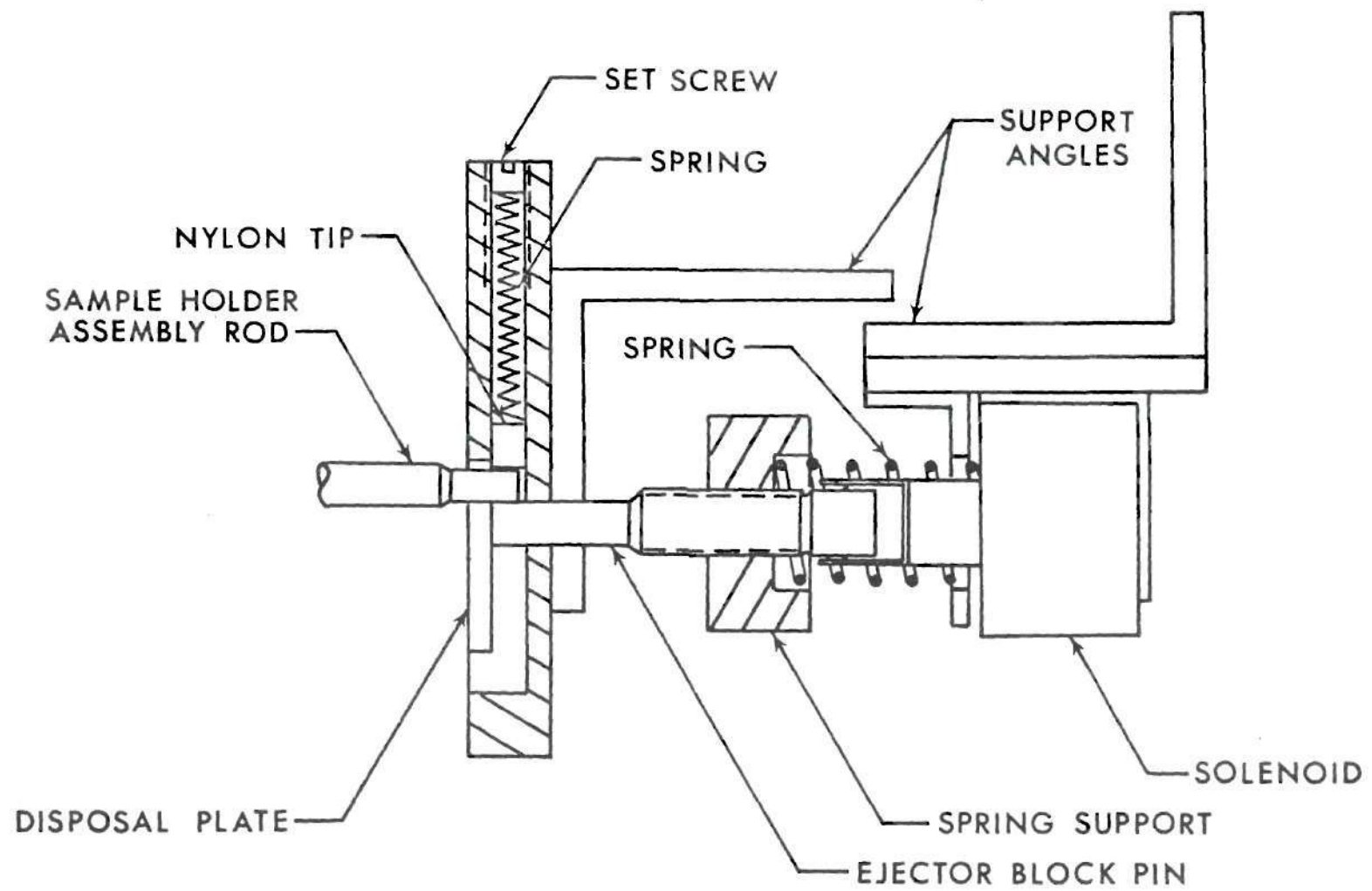


Figure A.3. Top View of the Ejector Assembly

APPENDIX B

SCHEMATICS OF THE LITA ELECTRICAL SYSTEM

This Appendix contains electrical schematics of the control panel, heater power system, preheat timer, and delay timer.

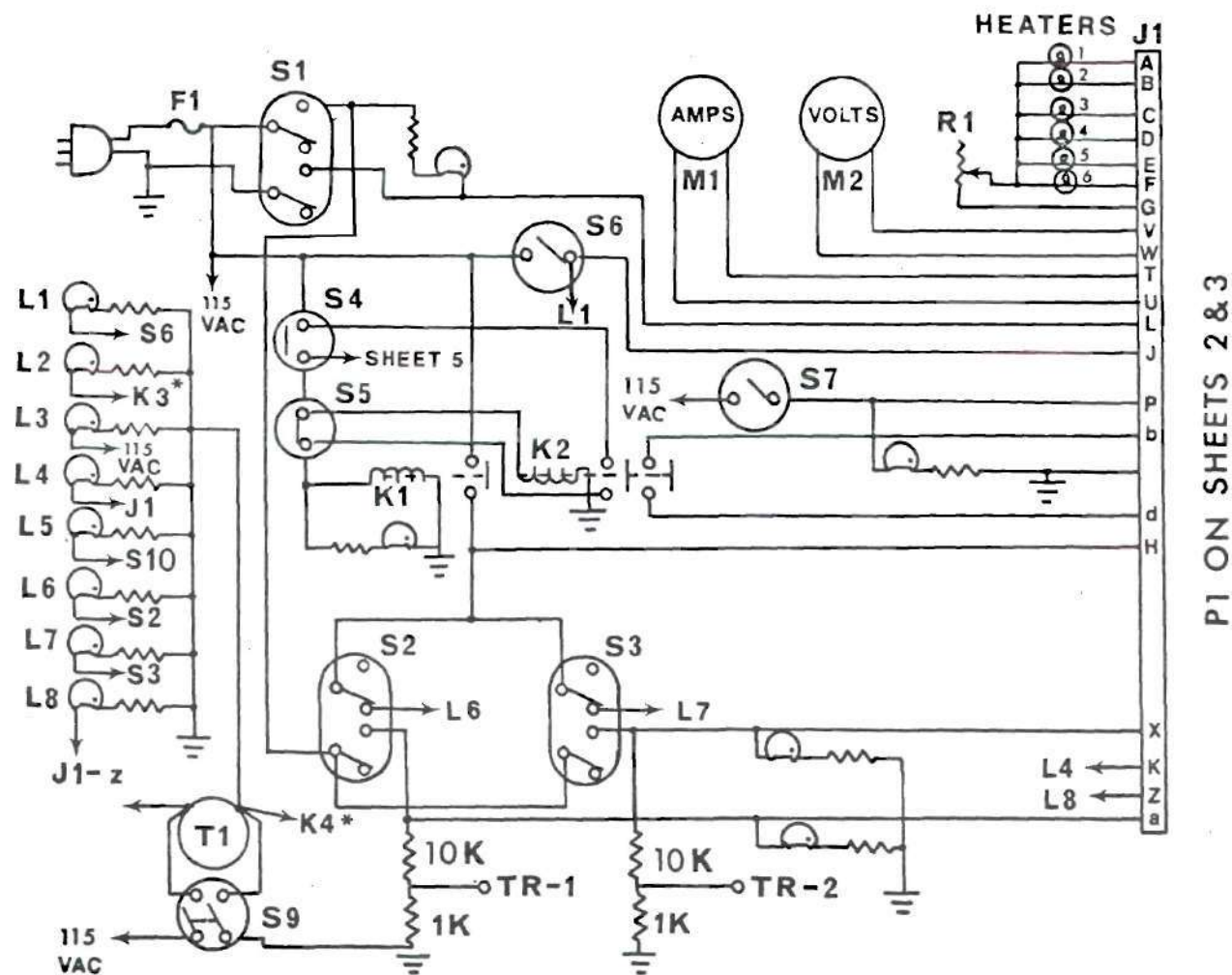


Figure B.1. Schematic of the Control Panel Electrical System (Sheet 1);
See Pages 94 and 95 for Key to Symbols; *See Figure B.2

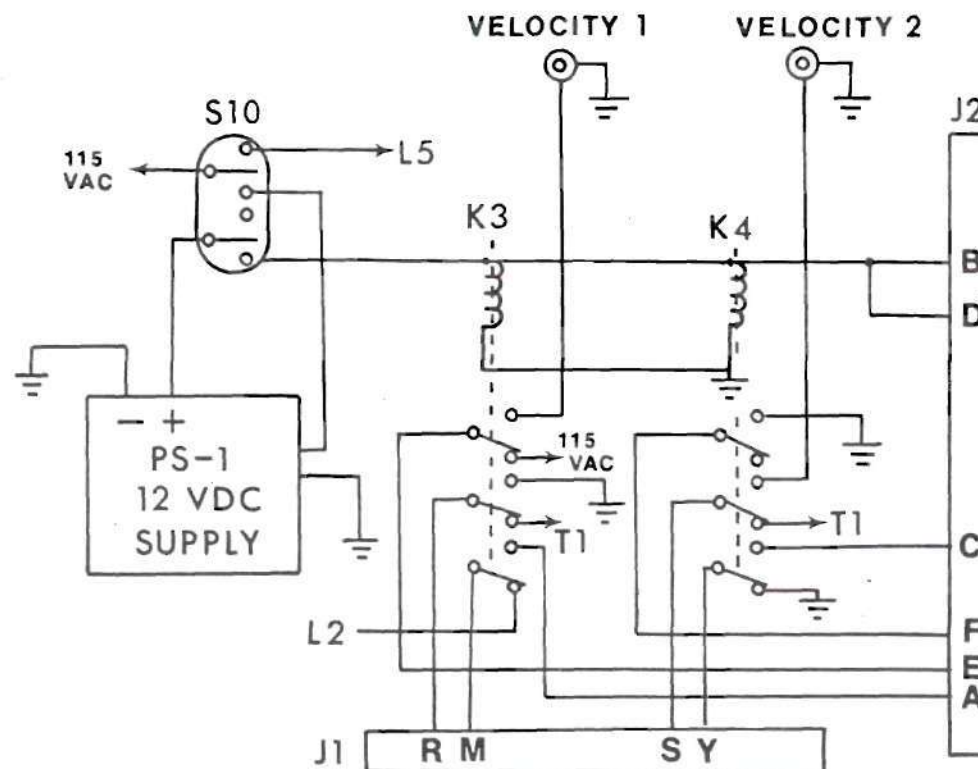


Figure B.2. Schematic of the Control Panel Electrical System (Sheet 2); See Pages 94 and 95 for Key to Symbols

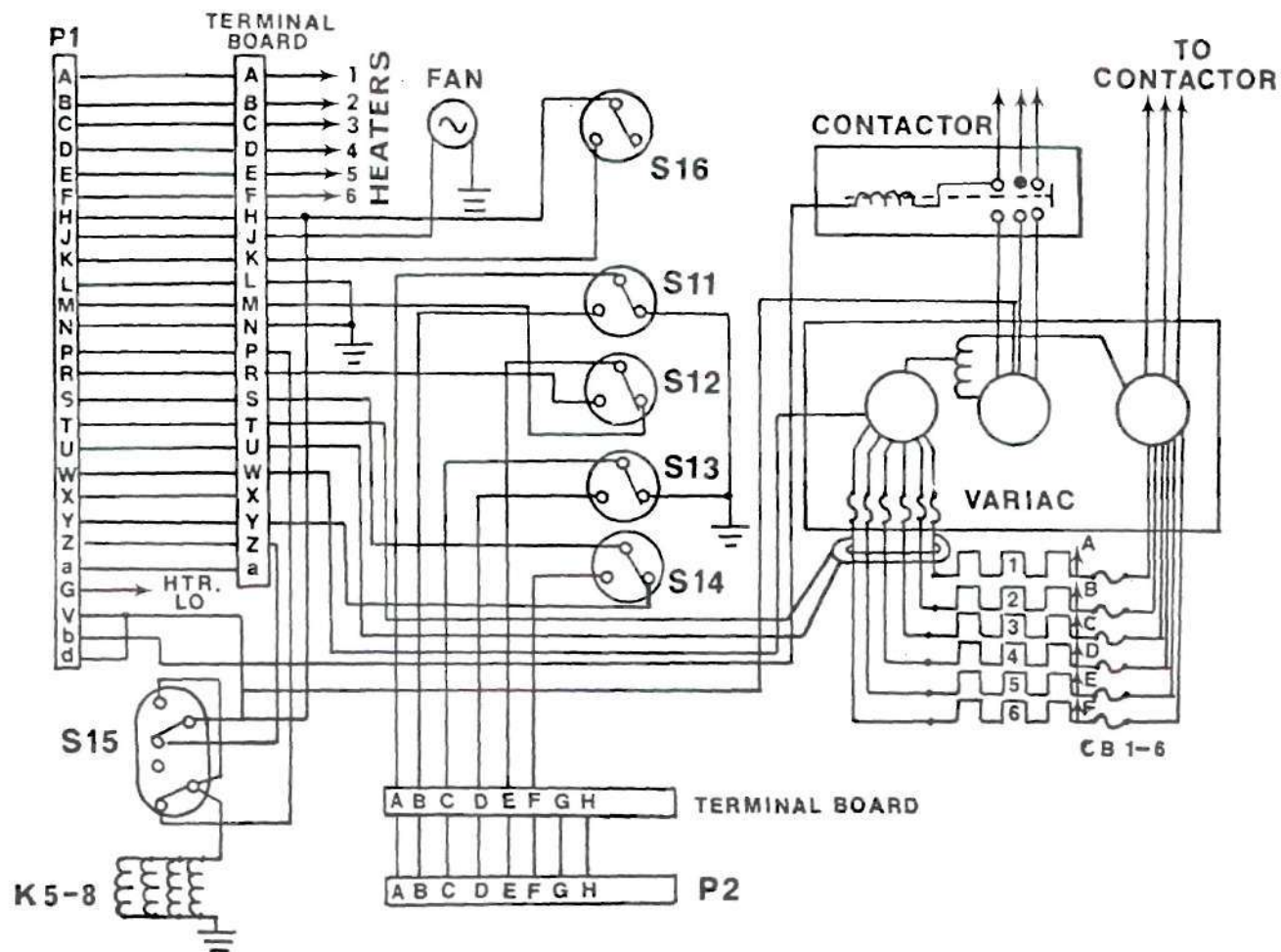


Figure B.3. Schematic of the LITA Power Supply System; See Pages 94 and 95 for Key to Symbols

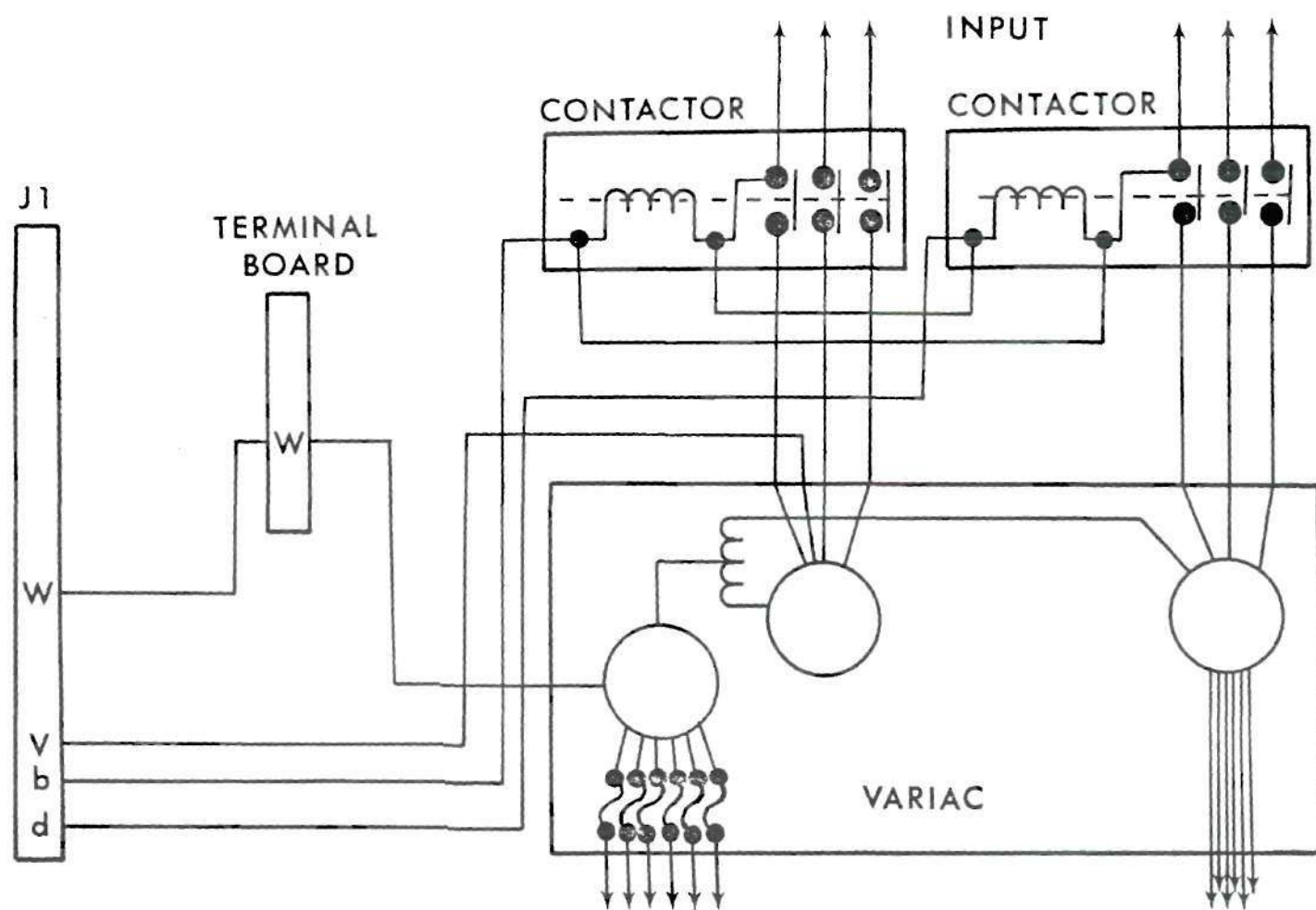


Figure B.4. Schematic of the Variac Power Supply; See Pages 94 and 95 for Key to Symbols

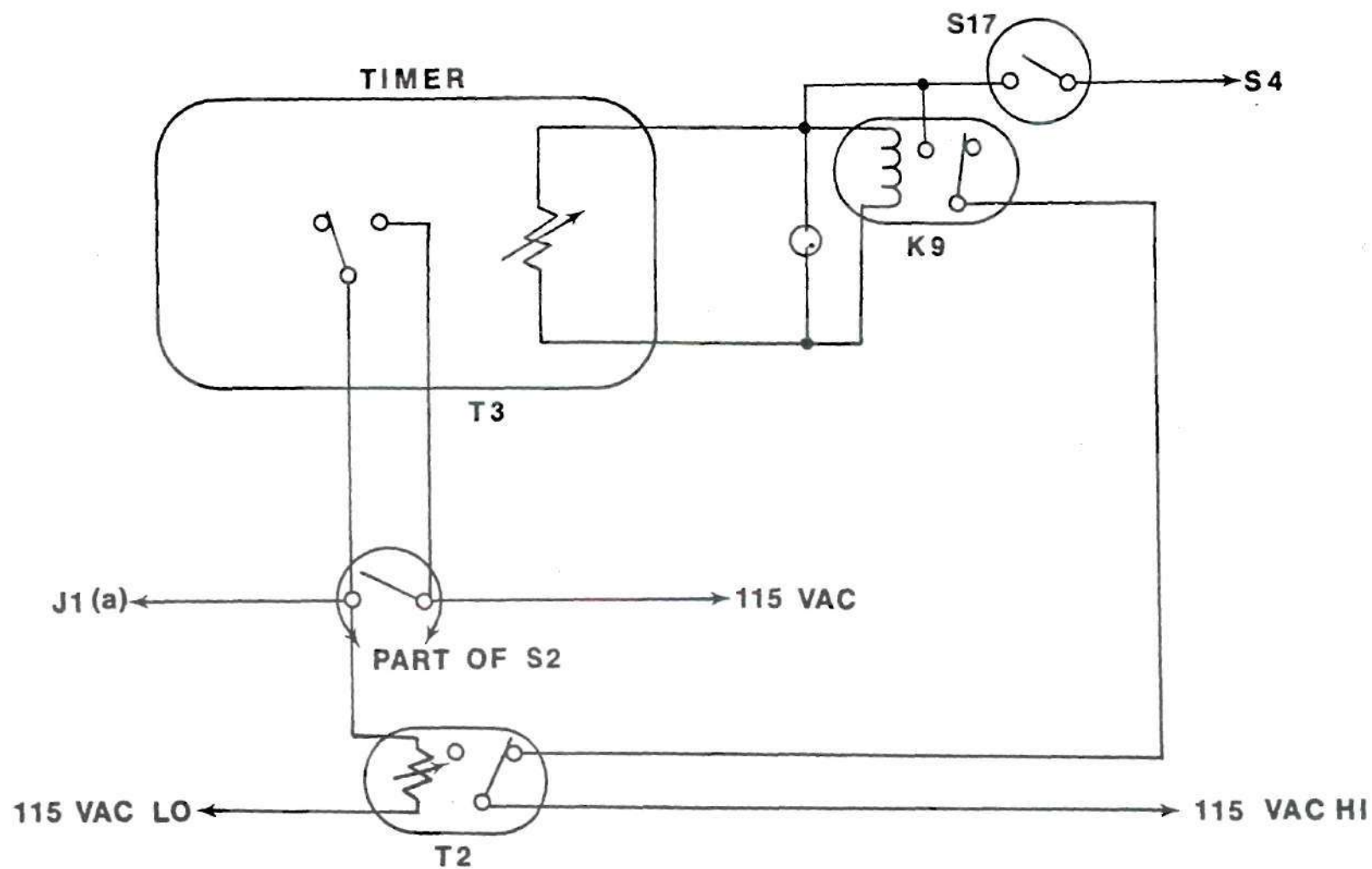


Figure B.5. Schematic of the Preheat Timer System; See Pages 94 and 95 for Key to Symbols

Key to Figures B.1-B.5

LITA Electrical System

Reference Designation	Description	Function
F1	Fuse, 20 amp	Protect control panel from overload
CB1-CB6	Breaker, 45 amp	To protect from overload on heaters 1 thru 6
S1	Toggle Switch, DPDT	Arming Sw
S2	Toggle Switch, DPDT	Shutter #1 control
S3	Toggle Switch, DPDT	Shutter #2 control
S4	Toggle Switch, SPST (N.O)	Master Power "ON"
S5	Toggle Switch, SPST (N.C.)	Master Power "OFF"
S6	Toggle Switch, SPST	Fan Control
S7	Toggle Switch, SPST	Disposal control
S8	Toggle Switch	Deleted
S9	Toggle Switch, DPST	Manual Timer Control
S10	Toggle Switch, DPDT Center off	Change micro-Sw function from exposure time to velocity test
S11	Micro Sw, SPDT	Shutter #1 vel. test pulse start
S12	Micro Sw, SPDT	Shutter #1, vel. test pulse stop
S13	Micro Sw, SPDT	Shutter #2 vel. test pulse start
S14	Micro Sw, SPDT	Shutter #3 vel. test pulse stop
S15	Toggle Switch, DPDT	Disposal load control mounted on shutter assembly
S16	Micro Sw, SPDT	To indicate blocking plate position
K1	Relay, 115 vac SPST	Apply power to status lamps and control Sw's
K2	Relay, 115 vac, DPST	Lock in control panel power and contactor for variac supply

Key to Figures B.1-B.5 (continued)

Reference Designation	Description	Function
K3,K4	Relay, 12 vdc, 4pdt	Energized position for velocity test
K5-8	Solenoids, 115 vac	To activate disposal interval
L1	Lamp. NE51H	Fan on when lit
L2	Lamp. NE51H	Micro Sw. #1 Ready
L3	Lamp. NE51H	Micro Sw. #2 Ready
L4	Lamp. NE51H	Shutter block stowed
L5	Lamp. NE51H	Sw. in exposure position
L6	Lamp. NE51H	Control Sw. for shutter #1 Off
L7	Lamp. NE51H	Control Sw. for shutter #2 Off
L8	Lamp. NE51H	Disposal Sw. Ready
T1	Timer, Display	To indicate exposure interval
T2	Timer, Delay	Adjust time of delay to retract shutter #1 actuator
R1	Rheostat	Control intensity of heater lamps
M1	Meter, Amp	Indicate heater current
M2	Meter, Volt	Indicate heater voltage
PS-1	Power Supply, 12 vdc	Supply voltage for vel./exp. relays and velocity signal.
VEL 1	Output Jack (UHF)	Velocity signal for shutter #1
VEL 2	Output Jack (UHF)	Velocity signal for shutter #1
TR-1	Output Jack	Trigger signal for shutter #1
TR-2	Output Jack	Trigger signal for shutter #2
T3	Timer, Preheat	Adjust preheat time from 1.5 to 30 seconds

APPENDIX C

FABRIC PROPERTIES AND DATA

This Appendix contains thermophysical properties of the fabrics tested. These properties are listed in References [6,7,8]. Also included in this Appendix are fabric ignition time data and typical infrascopes output history plots showing fabric ignition.

Table C.1. Thermophysical Properties of the Fabric
Samples Tested [6,7,8]

GIRCF No.	Classification and Color	Fiber Composition	(k/δ) (W/cm ² K)	c (W-s/g K)	$(\rho\delta)$ (mg/cm ²)	$\tilde{\rho}$	T_i (K)
16	Shirting, white	65/35% Polyester/Cotton	.015	1.50	13.14	.322	746
17	Batiste, white	65/35% Polyester/Cotton	.029	1.84	8.55	.255	753
18	Flannel, white	100% Cotton	.0075	1.735	12.85	.527	584
20	Flannel, navy blend	100% Wool	.0075	1.27	19.93	.105	753

Table C.2. Summary of Ignition Time Measurements
on Fabrics Samples Using LITA and RITA

GIRCFF No.	Incident Heat Flux (W/cm ²)	Ignition Time (s)		
		Mark I ³	LITA ¹ Temptron ⁴	RITA [6,7,8] ²
16	8.6	*	24.8	38.9
	10.8	14.4	12.3	18.5
	13.0	10.0	9.1	12.7
	15.8	8.8	7.6	9.4
17	7.8	*	54.8	69.5
	10.2	*	24.9	26.5
	15.7	8.2	6.5	7.2
	26.0	No Test	No Test	3.78
18	5.7	41.3	34.8	40.8
	6.8	No Test	No Test	23.8
	9.0	18.0	17.0	12.5
	14.3	9.6	*	6.8
	16.8	7.9	7.7	No Test
	18.8	No Test	No Test	4.7
20	8.6	6.2	6.2	17.7
	10.8	4.7	4.6	13.3
	13.0	3.72	3.87	10.9
	15.8	2.97	2.94	7.4
	16.8	2.8	2.6	No Test
**	6.4	32	*	No Test
	6.7	20.5	21	No Test
	6.7	23	21.5	No Test
	6.7	20	22	No Test
	9.6	15.8	*	No Test

¹ 15.2 cm x 15.2 cm sample

² 2.5 cm diameter sample

³ Focused at 5 cm from the bottom of the sample

⁴ Focused at 13.5 cm from the bottom of the sample

* No data

** 100 percent cotton fabric, obtained from the School
of Textile Engineering, Georgia Institute of Technology

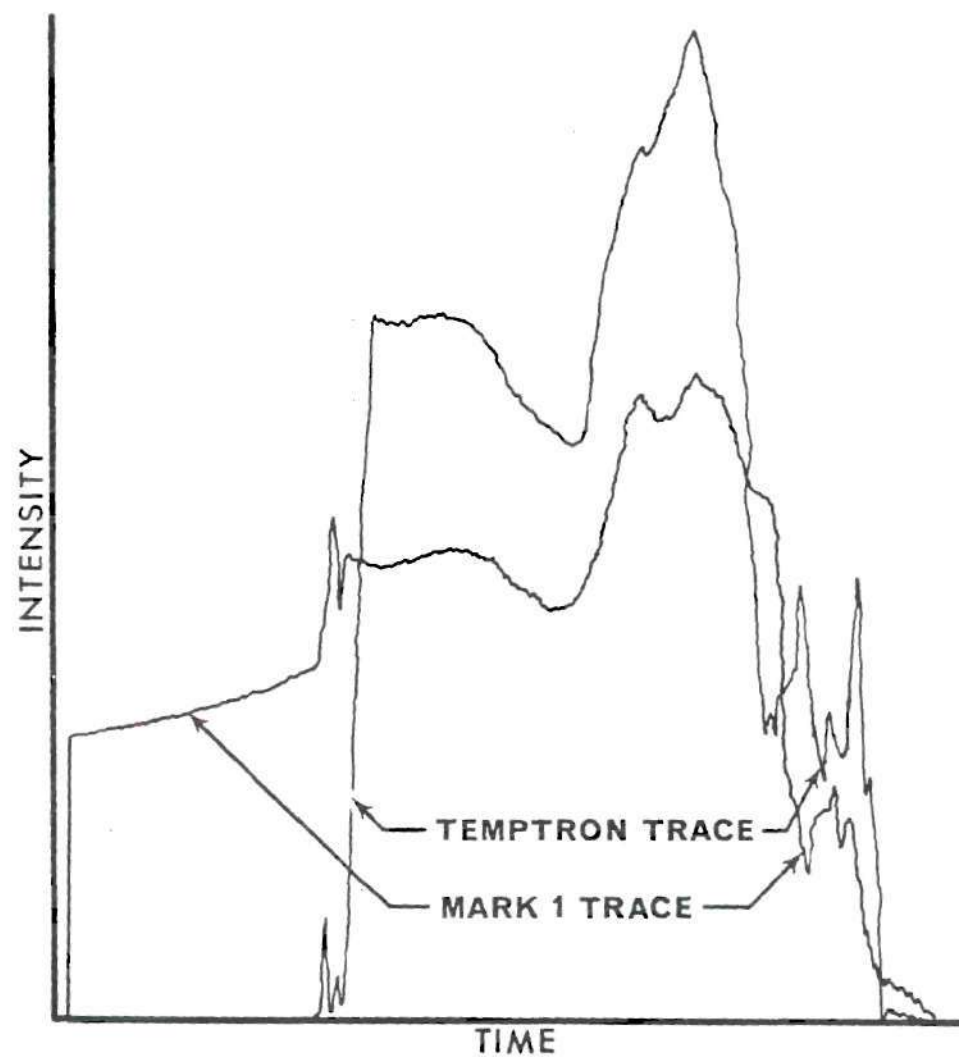


Figure C.1. Infrascopes Output History Plots; GIRCFF Fabric Number 20 Exposed to an Incident Heat Flux of 15.8 W/cm^2 ; Temptron Focused at 13.5 cm and Mark I at 5.0 cm above the Bottom Edge of the Sample

APPENDIX D

WOOD PROPERTIES AND DATA

This Appendix contains thermophysical properties of the wood samples tested. The self-ignition temperatures, T_i , are equated to the self-ignition temperature of cellulosic materials obtained from Reference [9]. The reflectance, $\tilde{\rho}$, is equated to the solar radiation reflectance of oak obtained from Reference [10] divided by 1.14. (The divisor is equal to the ratio of the reflectances of charred and uncharred samples of cotton fabric, GIRCFF number 18, obtained from References [6,7,8].) The sample thickness, δ , is the mean value of the samples tested. The remaining thermophysical properties were obtained from Reference [11].

Also included in this Appendix are the wood ignition time test data and typical infrascopes output history plots showing wood ignition.

Table D.1. Thermophysical Properties of the Wood Samples Tested [6,7,8,9,10,11]

Description	δ (cm)	ρ (g/cm ³)	k/δ (W/cm ² K)	c (W-s/gk)	$\tilde{\rho}$	T_i (K)
Plywood, 1/4"	.61	.545	.00181	1.2	.25	798
Plywood, 1/2"	1.26	.545	.00904	1.2	.25	798
Plywood, 3/4"	1.84	.545	.00605	1.2	.25	798
Western Fir, 3/4"	1.89	.513	.00599	1.4	.25	798

Table D.2. Summary of Ignition Time Measurements
on Thermally Thick Materials, 15.2 cm
x 15.2 cm Samples

Material	Incident Heat Flux (W/cm ²)	Ignition Time (s)	
		Mark I ¹	Temptron ²
Western Fir, 3/4"	6.0	*	*
	8.0	42.6	42.9
	8.0	46.3	46.3
	12.0	**	16.5
	14.0	14.1	13.2
	16.8	11.6	11.6
Plywood, 1/4"	6.0	100	100
	8.0	59.1	58.9
	12.0	29.4	29.4
	12.0	19.0	20.4
	12.0	23.1	23.1
	12.0	25.2	25.2
	14.0	20.2	20.2
	16.8	No Test	No Test
Plywood, 1/2"	6.0	*	*
	6.0	**	91.3
	8.0	46.8	46.6
	8.0	47.4	47.4
	12.0	25.0	24.9
	14.0	17.8	18.0
	16.8	**	15.0
Plywood, 3/4"	6.0	81.9	81.9
	8.0	52.3	52.3
	12.0	24.0	23.8
	14.0	17.4	17.4
	16.8	14.2	14.8
	16.8	**	13.5

¹Focused at 5 cm from the bottom of the sample

²Focused at 13.5 cm from the bottom of the sample

* No ignition recorded or visually observed

** No data

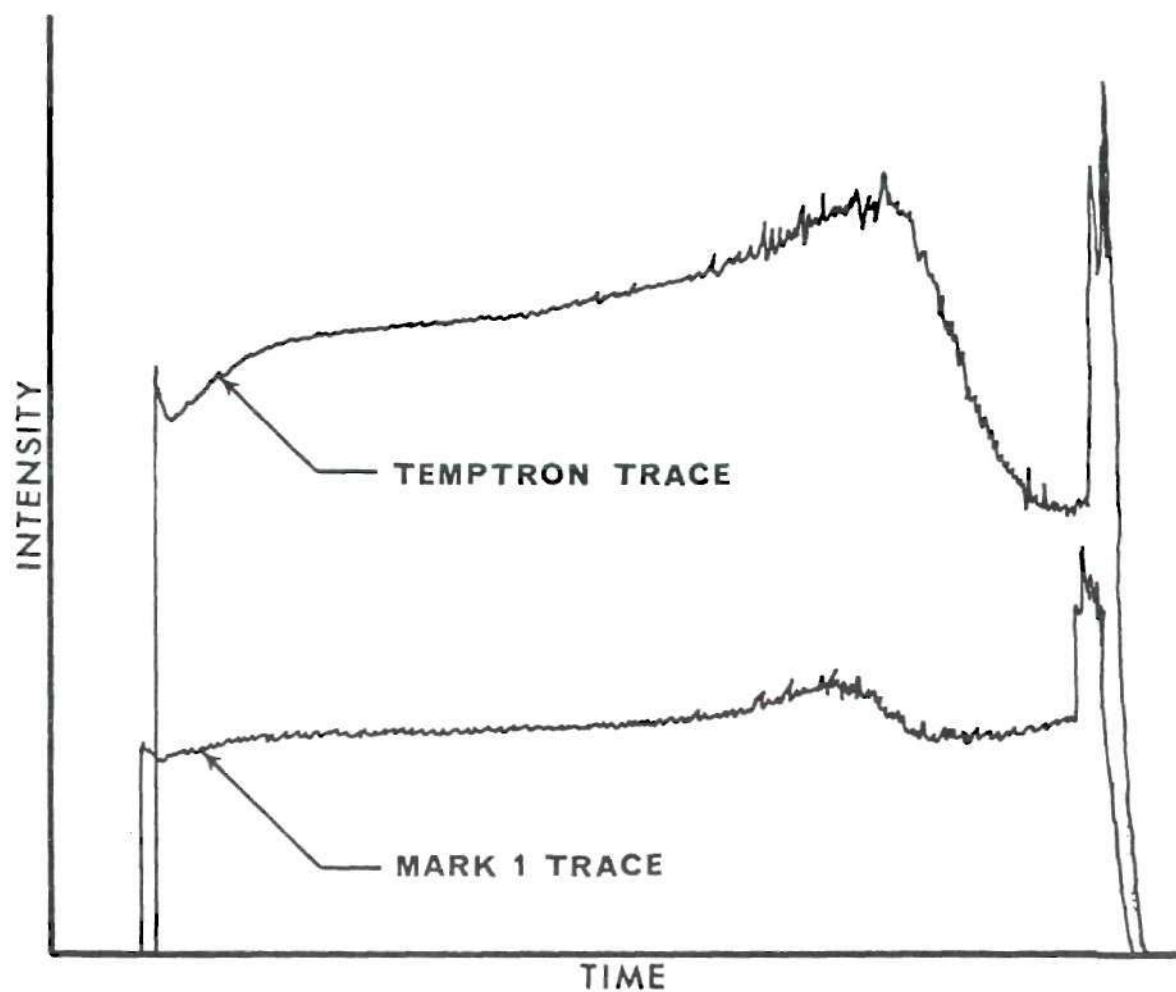


Figure D.1. Infrascope Output History Plots; 1/2 Inch Plywood Exposed to an Incident Heat Flux of 8.0 W/cm^2 ; Temptron Focused at 13.5 cm and Mark I Focused at 5.0 cm above the Bottom Edge of the Sample

APPENDIX E

OPERATING CHARACTERISTICS OF THE RADIANT HEATER STACK

This Appendix contains operating characteristics of the radiant heater stack. Table E.1 lists heater current versus heater voltage. Figure E.1 is a plot of steady state incident heat flux and preheat time versus idle heater voltage.

Table E.1. Total Heater Current Versus Heater Voltage

Total Current (A)	Heater Voltage-Idle (V)	Heater Voltage-Load (V)
100	50	48
110	60	58
118	70	68
125	80	76
134	90	85
142	100	95
148	110	105
157	120	115
163	130	125
171	140	135
176	150	143
183	160	153
189	170	163
196	180	173
201	190	183
206	200	193
209	204	197

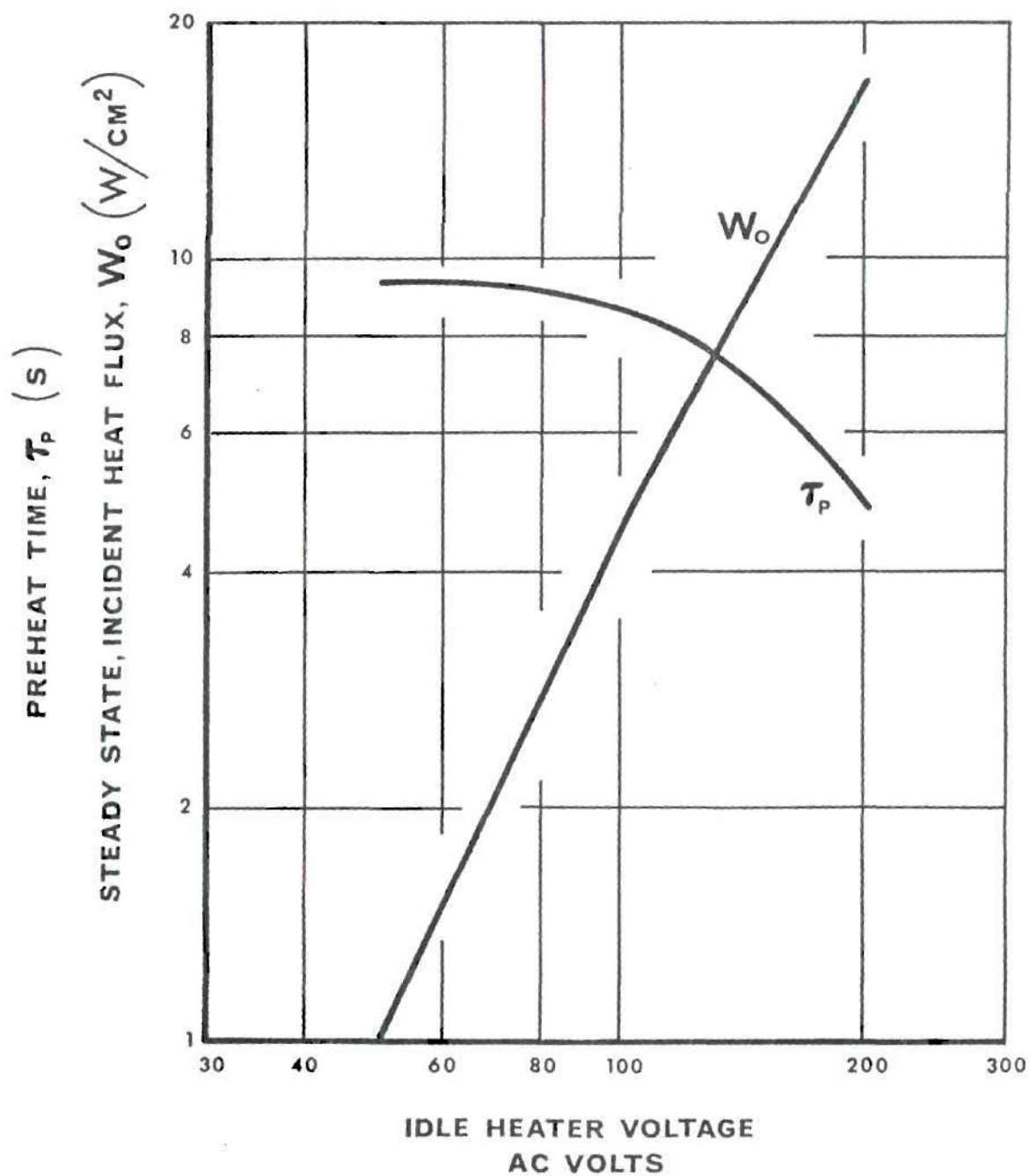


Figure E.1. Steady State, Incident Heat Flux and Preheat Time Versus Idle Heater Voltage

BIBLIOGRAPHY

1. "America Burning," National Commission on Fire Prevention and Control, U. S. Government Printing Office, Washington D. C., Stock Number 5200-00004, May, 1973.
2. "The Flammable Fabrics Program," NBS Technical Note 596, National Bureau of Standards, Washington, D. C., 1970.
3. Government-Industry Research Committee on Fabric Flammability, "Study of Hazards from Burning Apparel and the Relation of Hazards to Test Methods," A statement prepared by the Research Committee, Dr. E. Passaglia, Chairman, National Bureau of Standards, June 5, 1970.
4. Tribus, M., "Decision Analysis Approach to Satisfying the Requirements of the Flammable Fabrics Act," Paper presented at the Textile and Needle Trades Division, American Society of Quality Control, Greensboro, North Carolina, February 2, 1970.
5. Alkidas, A., Hess, R. W., Wulff, W. and Zuber, N., "Study of Hazards from Burning Apparel and the Relation of Hazards to Test Methods," First Annual Report, NSF Grant No. GK-27189, School of Mechanical Engineering, Georgia Institute of Technology, Atlanta, Georgia, December, 1971, NTIS Document No. COM-73-10954.
6. Durbetaki, P., Wulff, et al., "Study of Hazards from Burning Apparel and the Relation of Hazards to Test Methods," Second Annual Report, NSF Grant No. GI-31882, School of Mechanical Engineering, Georgia Institute of Technology, Atlanta, Georgia, December, 1972, NTIS Document No. PB-242-597/AS.
7. Wulff, W., Alkidas, A., Hess, R. W. and Zuber, N., "Fabric Ignition," Textile Research Journal, 43, 580-584, (1973).
8. Wulff, W., Zuber, N., Alkidas, A. and Hess, R. W., "Ignition of Fabrics Under Radiative Heating," Combustion Science and Technology, 6, 321-334, (1973).

9. Sims, D. L., "Ignition of Cellulosic Materials by Radiation," Combustion and Flame, 4, p. 299, (1972).
10. Gebhart, Benjamin, Heat Transfer, McGraw-Hill, Inc., New York, 1961.
11. ASHRAE Handbook, George Banton Co., Menasha, Wisconsin, 1972.